FABRICATION OF THERMO-RESPONSIVE MEMBRANES AND APPLICATION

FABRICATION OF PAPER BASED THERMO-RESPONSIVE MEMBRANES AND INVESTIGATION FOR THEIR USE IN ADSORPTION OF EMERGING WATER CONTAMINANTS

By

EVAN MAH, B.Sc.

A Thesis

Submitted to the School of Graduate Studies

in Partial Fulfillment of the Requirements

for the Degree

Master of Applied Science

McMaster University

DESCRIPTIVE NOTES

MASTER OF APPLIED SCIENCE (2012) McMaster University
(Chemical Engineering) Hamilton, ON

TITLE: Paper Based Thermo-responsive Membranes for Reversible Adsorption of Estrogens from Wastewater

AUTHOR: Evan Mah, B.Sc. (Queen's University)

SUPERVISOR: Dr. R. Ghosh
Dr. R. Pelton

NUMBER OF PAGES: viii, 64

Abstract

Endocrine disrupting substances such as oestrogen hormones have been frequently reported to exist in potent concentrations in wastewater treatment plant effluent and other surface waters. Common techniques of wastewater treatment have varied effectiveness to remove estrogens from wastewater. A thermo-responsive smart membrane technology is investigated for its use in adsorptive removal of 17β-estradiol, as a model oestrogen, from a background electrolyte solution. A simplified fabrication method is adapted for hydrogel-substrate composite thermo-responsive membranes. Deposition of hydrogel occurs through aqueous polymerization in a coating process dissimilar to common grafting techniques. Acrylamide and acrylic acid monomers are polymerized in two different structures, a random copolymer as well as an interpenetrating network, to form a positive volume-phase transition hydrogel coating. Subsequent membranes experience high permeability at low temperatures with a gating mechanism reducing permeability upon heating. The effects of crosslinker content, monomer ratio, mass loading and butylmethacrylate content are investigate. Only mass loading was found to have significant influence on the behaviour of the membranes in all cases. The variations of the other factors were too little to have great influence. The membranes with the most stable permeability response function were then used in 17β-estradiol adsorption tests, investigating the binding capacity at both colder water temperatures (10^{o}C) and warmer water temperatures (40^{o}C). In the collapse and swelling of the volume-phase transitions, the membranes changed their solution properties which were hypothesized to also alter surface functionality. After introducing the estradiol sample, the membranes were subjected to temperature change with the expectation that any bound material would elute once the surface functionality of the membranes became adequately altered. Only some membranes produced an elution fraction while others appeared to undergo irreversible binding with a possible delayed elution. Removal of dosed 17β-estradiol is reported as adsorbed mass per area of membrane. IPN coated membranes generally outperformed random copolymer coated membranes. Wet tensile strength and ESEM imaging are also used to characterise these membranes. The results of this work demonstrate the ability of a thermo-responsive membrane to radically change its size and solution properties to provide sufficient interface functionality for reversible binding of hydrophobic compounds. Although not observed consistently, it is probable that, through optimization of coating chemistry, the reversible adsorption of compound by a thermo-responsive membrane is viable.

Acknowledgements

My first and foremost acknowledgements must go to my supervisors, Dr. Raja Ghosh and Dr. Robert Pelton, without whom my research would have taken much longer to gain direction and substance. The critical inputs from both supervisors have been vital for my continued motivation to improve the quality of my work, both on paper and in the lab. Understanding and support through injury and illness along with the amazing academic opportunities provided such as conferences and journal manuscript writing have made my graduate student experience fulfilling and unforgettable.

I would like to thank the Chemical Engineering Department and all the administrative staff who have made it easier to work at a large institution with many difference policies and procedures, specifically Sally Watson, Linn Falkner, Melissa Vasil, Kathy Goodram and Nanci Cole. Being co-supervised has made it possible for me to use the combined knowledge and support of two graduate student groups, the McMaster Bioseparations Engineering Research Group under Dr. Ghosh and the SENTINEL Bioactive Paper research group under Dr. Pelton. Students in both groups have my sincerest gratitude for teaching me new skills and making the work environment a friendly place. MBERG has especially been enjoyable as it was with them; Seungmi, Annabel, Pans, Rahul, Pedrom, Yusra, Simon, Steve, and Ryan; that I spent the most time and learned the most from. I would also like to acknowledge the hard work of Paul Gatt, Dan Wright and Doug Keller who helped resolve many of my lab equipment problems. Klaus Schultes at the Life Sciences Microscopy Lab should also be recognized for the training and technical knowledge provided on the ESEM.

I would like to draw recognition to the SENTINEL Bioactive Paper Network that provided funding for the work contained herein. Without the support of this agency and its various meetings and industry acumen, this would not have been possible.

Finally I would like to express my deepest gratitude to my family and loved ones, primarily my parents and grandparents who have encouraged me to find success in life wherever I may find it and so have accepted my decisions to do so far away from home. I understand it is especially hard on them as they are not always able to witness the results of their love and support because of the distance and I am not always able to give them any support they may need from me. Thank-you to Maria, my friend and love, for all of her patience and sacrifice while waiting for me to finish.

Table of Contents

1. Introduction 1
1.1 Water Contaminants 1
1.2 Smart Membranes 3
1.3 Positive Thermo-Responsive Membranes 4
1.4 Hypothesis 4
1.5 Thesis Outline 5
1.6 Chapter References 7
2. Positive Thermo-responsive Hydrogels for Application with Smart Membranes 12
2.1 Polysulfobetaine Hydrogels 12
2.1.1 Polysulfobetaine Smart Membranes 14
2.2 Acrylamide Based Hydrogels 16
2.2.1 Interacting Forces 17
2.2.2 Hydrogel Synthesis 19
2.2.3 Introducing Hydrophobic Content 23
2.2.4 Stabilizing Am-AA Complexation 25
2.3 Novel PVT Hydrogels 26
2.4 Review and Analysis 28
2.5 Chapter References 29
3. Experimental Setup 34
3.1 Materials 34
3.2 Preparation of Hydrogel Coated Paper Discs 34
3.2.1 Random Copolymer Coatings 34
3.2.2 Interpenetrating Network Coatings 36
3.2.3 Mass Gain 36
3.3 Hydraulic Permeability Testing 37
3.3.1 Permeability Calculation 37
3.4 Adsorption (Binding) Test Procedure 38
3.4.1 Background Electrolyte Buffer Preparation 38
3.4.2 Injection Sample Preparation 39
3.4.3 Hormone binding 39
3.5 Environmental Scanning Electron Microscope (ESEM) Imaging 39
3.6 Wet Strength Testing 39
3.7 Chapter References 40
4. Results & Discussion 41

4.1 Synthesis and characterization of paper membranes coated with thermo-responsive hydrogels 41
4.1.1 Series A Membranes 41
4.1.2 Series B Membranes 45
4.2 Estradiol adsorption potential of thermo-responsive membranes in low salt solution 48
4.2.1 Membrane Behaviour and Effect of Module Selection 48
4.2.2 Estradiol Adsorption 49
4.2.3 Insulin Adsorption 54
4.3 ESEM Imaging 55
4.4 Wet Tensile Testing 56
4.5 Chapter References 57
5. Conclusion 59
5.1 Membrane Coating Synthesis 59
5.2 Adsorption Testing 60
5.3 Result Evaluation 61
5.3.1 Additional Remarks 61
5.4 Recommendations 62
5.5 Chapter References 63

List of Figures

Molecular structure of 17β-estradiol. 5
Sulfobetaine functional unit 12
Effect of polymer concentration and salt on polySPE phase behaviour with respect to temperature. ■, Polymer $M_w = 4.35x10^5$; ▲, Salt water (0.51 M NaCl) [8] 13
Short zwitterionic cluster (A), intragroup ion pair (B), long zwitterionic cluster (C), nucleated from a short cluster with entropy driven propagation outwards. Figure adopted from [13]. 15
Competing hydrogen bond complexations in PAm and PAA hydrogels. Adapted with permission from [30]. Copyright 1994 American Chemical Society. 17
Hysteresis as observed by light transmittance characteristic of many Am-AA based hydrogels [39]. 19
Chemical similarities between acrylamide, acrylic acid and N'-methylene bisacrylamide. 20
Scanning electron microscope image of nylon-6 membrane after sequential polymerization of a Am-AA IPN [49]. 22
Micellular crosslinks of OP7-AC and SDS. Reprinted with permission from [35]. Copyright 2010 American Chemical Society. 24

Effect of DMAm content on poly(DMAm-co-Am)/PAA IPN (A). Percentages are by mol. Complexation of PDAm with PAA (B). Adapted with permission from [30]. Copyright 1994 American Chemical Society. 26
N-Acryloyl glycinamide 26
N-Acryloylasparaginamide 28
Equipment diagram for membrane adsorption....38
A-Series membrane coating polymerization results. Dry mass gain shown only. 41
Permeability profile of uncoated Whatman grade 5 filter paper through two temperature cycles at an elevated water flux. 42
Permeability of A1-1 coating formulation, adapted from Zhou et al., through three temperature cycles. 42
Hydrogen bonding between the amide and carboxyl groups of acrylamide and acrylic acid....44
B-series coated membrane polymerization results. Dry and wet mass gains. 46
Comparative plots of permeability response to temperature for membranes B1-1 and B3-2 for both a stirred cell module and a dead-end stack module. 49
E2 retained by each membrane at cold temperatures, normalized to membrane area....50
E2 retained by each membrane at hot temperatures, normalized to membrane area. 51
E2 flow-through UV absorbance signals. Shown are both the first and second cold state flow-through for coated membranes B1-1 (1A/B), B3-1 (2A/B) and B3-2 (3A/B). Membrane B1-1 shows significant peak widening while B3-1 and B3-2 both display an elution fraction. The integration baselines for the flow-through fractions are shown and E2 injection occurs at time = 0. A control UV absorbance signal for uncoated paper is provided in light grey for comparison in each graph. 52
Insulin retained by each membrane at cold temperatures, normalized to membrane area. 54
Insulin retained by each membrane at hot temperatures, normalized to membrane area. 54
Insulin flow-through UV absorbance profiles for membranes B1-1 and B3-2. Both cold (a) and hot (b) temperature signals are shown for each membrane. Small elution fractions are identifiable for B1-1 a, and both B3-2 temperature conditions. The integration baselines are shown for the flow through fractions and E2 injection occurs at time = 0. A control UV absorbance signal for uncoated paper is provided in light grey for comparison in each graph. 55
ESEM images of various membranes. Shown are: dry (A) and wet (B) uncoated Whatman filter paper; paper substrate coated with pre-gel formula A4-1, 10.96% mass gain, dry conditions (C) and wet conditions (D); paper substrate coated with pre-gel formula B2-1, 11.84% mass gain, dry conditions (E) and wet conditions (F); paper substrate coated with pre-gel formula B3-1, 9.33% mass gain, dry conditions (G) and wet conditions (H). All scale bars measure 150 µm. 56

List of Tables

Various recipes for Am-AA based hydrogels 21
Various recipes for hydrogels incorporating hydrophobic monomer 23

Feed compositions for random copolymer coatings in series A. 35
Feed composition for random copolymer coatings in series B. 35
Feed compositions for IPN coatings in series A and B. 36
Summary of permeability for random copolymer coated membrane in Series A. 43
Summary of permeability for IPN coated membranes in Series A. 45
Summary of permeability for coated membranes in Series B. 47
Mass loading of hydrogel on membranes for adsorption testing. 49
Results of wet tensile strength testing of various coated membranes. 57

List of Abbreviations and Symbols

AA – Acrylic acid
Am – Acrylamide
ATRP – Atom-transfer radical polymerization
BMA – Butyl methacrylate
E1 – Estrone
E2 – 17β-estradiol
EE2 – 17α-ethinylestradiol
EDS – Endocrine distrupting substance
IPN – Interpenetrating network
K_{ow} – Octanol-water partition coefficient
MBAm – N,N'-methylene bis-acrylamide
NAAm – N-Acryloyl asparaginamide
NAcAm – N-acetyl acrylamide
NAGA – Poly (N-acryloyl glycinamide)
NF – Nanofiltration
NIPAm – Poly (N-isopropyl acrylamide)
NVT – Negative volume-phase transition
PVT – Positive volume-phase transition
RO – Reverse osmosis
VPTT – Volume-phase transition temperature
WWTP – Wastewater treatment plant

J_v – hydraulic flux ($m^3 \cdot [m^2 \cdot s]^{-1}$)
κ – Darcy's law permeability (m^2)
$\bar{\kappa}$ – the mean Darcy permeability (m^2)
ℓ – the thickness of the membrane (m)
m – mass (g)
μ(T) – dynamic viscosity as a function of temperature (Pa·s)
$\bar{T}$ – the mean temperature (^oC)
TMP – transmembrane pressure change (Pa)

1. Introduction

1.1 Water Contaminants

There is an emerging source of environmental contaminants from consumer goods under the label, pharmaceuticals and personal care products. This group of products contributes a wide range of chemical contaminants into soils and waterways that threaten drinking water quality and the function of ecosystems [1-3]. Pharmaceutical substances include any active drug agents while personal care products can be more difficult to identify but primary contaminants in this group include anti-bacterial preservation chemicals like triclosan, cleaning agent surfactants like nonylphenol and common active food-stuff chemicals like caffeine. These contaminants have varied toxic impacts on ecosystems and are effective at equally varied concentrations. While some chemicals, particularly pesticides and certain pharmaceuticals, have specific origins such as hospitals, veterinary clinics and agricultural run-off, most others enter the environment across municipalities in well dispersed occurrences [4]. Contaminants from an easily identified, continual source are more easily mitigated at that source [5]. For the many other contaminants that originate from a non-uniform mixture of residential and commercial sources, mitigation can only easily occur at concentration points such as wastewater treatment plants (WWTPs) [6]. Degradation or removal of pharmaceutical contaminants at WWTPs can happen at any stage but are most likely to occur in activated sludge systems, biological nutrient removal systems, or during ozonation/irradiation disinfection [1, 7-9]. Some pharmaceutical agents are persistent enough to withstand these treatments and not all WWTPs are equipped with treatment systems proficient at removing pharmaceutical contaminants. Persistent compounds are commonly also endocrine disrupting substances (EDSs). These are chemicals that can influence hormonal and reproductive functions in humans and many animal species [3]. Potent EDSs negate the requirement of high environmental persistency as they are still effective at very low concentrations. Most prominent among these highly potent EDSs are oestrogen and progestin hormones, specifically oestrone (E1), 17β-estradiol (E2), 17α-ethinylestradiol (EE3) which enter wastewater by human excretion [10-13]. Specifically, E2 and EE2 have the highest potency, environmental persistence and are present in environment waters at effective concentrations [13]. Studies have found E2 levels as high as 200 ng/L in US surface waters [14], 64 ng/L and 3 ng/L in Canadian and German municipal wastewater treatment plant effluents, respectively [15], and 2.3 ng/L in various EU drinking water sources [16, 17]. Not only is E2 active in humans at the ng/L level [18, 19], but also in wild fish. Concentrations as low as 1-4 ng/L have been shown to cause partial or complete feminisation of males in certain fish species [20-22]. Estrogens are stable compounds in

water which leads to their highly variable removal. Differences in season and the natural organic matter content of wastewater gives rise to variation in E2 removal efficiency between 39-98% by activated sludge processes [8, 9].

There are several supplemental methods that have been examined to aid in the removal of estrogens at WWTPs, particularly composite oxidation, trickling filters, activated carbon and membrane filters. Trickling filters are generally poor at removing oestrogen [9, 15]. Each other method varies in effectiveness and there is not a clearly superior method for reducing emerging contaminants [7]. Chlorine, ozone and UV-light have high reduction efficiencies of persistent hormone compounds in wastewater, however little is known about the effects of the products and metabolites that are produced, possibly creating the same toxic problems but with other compounds. Membrane filters and activated carbon have similar issues in that both remove the contaminants from wastewater but don't degrade them, making a secondary degradation process necessary. Activated carbon poses additional challenges for disposal and regeneration due to its powdered or granulated form and high dosage requirement [23]. Membrane filters in commercial wastewater treatment are a relatively emerging technology. Membrane technologies have been shown to be very effective at removal of estrogens from aqueous media. Investigative studies for oestrogen removal often utilize nanofiltration (NF) and reverse osmosis (RO) membranes as it is hypothesized that steric exclusion plays a dominant role due to the small size of the hormones. However it was been determined that size exclusion is only a dominant interaction for very small pore membranes and only after the adsorption equilibrium has been reached [24-28]. Membrane oestrogen removal techniques are therefore most effective as adsorption processes with a few exceptions [24, 26]. Hydrogen bonding or hydrophobic interactions are the two most hypothesized contributing driving forces for adsorption. Electrostatic interactions are dismissed as the pH required for deprotonation of estrogens is quite high. A decreasing retention behaviour typical of site-specific adsorption as well as available hydroxyl groups on E2 make a case for hydrogen bonding while a high octanol-water partition coefficient does the same for hydrophobic interaction [24, 28, 29]. NF and RO membranes can achieve high removal efficiencies for E2 but they demand high transmembrane pressures (TMP) to do so at meaningful liquid flux which often makes them financially demanding [25, 30-32]. Since it has been determined to typically be an adsorption driven process, it is logical to instead evaluate membrane adsorption techniques with microfiltration membranes, which are capable of much higher fluxes at lower TMP. Adsorptive membranes with high enough hydrogen bonding or hydrophobic interaction adsorption capacities may be able to achieve comparable oestrogen removal rates to UF, NF and RO membranes [24]. In this instance, material selection or surface modification could be used to modify the interfacial characteristics of a membrane. However, by simply inducing stronger hydrogen bonding or hydrophobic

interaction capability, it would create a single use technology that would require replacement and disposal once saturated. This presents an opportunity for adsorptive membranes that can easily be recharged several times. Smart membranes are an emerging, stimuli-responsive technology that are widely replacing traditional membranes in academic studies, especially in areas like membrane chromatography and controlled release of drugs, due to their improved or expanded function [33-37]. They may like-wise provide a better solution for removal of oestrogen and other EDSs from wastewater than traditional membranes.

1.2 Smart Membranes

By applying an adaptive property to a sedentary membrane, a membrane's utility or productivity or both may be improved. Inspired by this concept, stimuli-responsive membranes are becoming increasingly prevalent in membrane research. These "smart" membranes typically have one or more characteristics that are stimuli-responsive, able to change physical or chemical attributes reversibly. This responsive function can be employed either reactively or on command. For membranes employed in processes that make use of aqueous based solvents, certain hydrogels can be formed into a membrane, or combined with a membrane substrate to create an environmentally adaptive technology [33, 34]. Gel membranes lacking a substrate often have poor mechanical strength and have limited use. Hydrogels are water-soluble polymer gels that, instead of dissolving, entrap water in the interstitial spaces between polymer segments. Hydrophilic pendant groups like alcohols, carboxylic acids and amides are what enable the gels to be water-soluble. There are several forms of stimuli that will invoke a response from certain hydrogels such as temperature [38-40], electric fields [41, 42], solvent composition [43, 44], ionic strength [37, 45], pH [46, 47] and interaction with analytes [48, 49]. Substrates are generally cellulose derivatives or several of the major synthetic polymers like polypropylene and polyethylene. Choice of substrate material is made based on required tortuosity, porosity, pore size distribution, chemical functionality and tendency for uncontrolled adsorption of particles [34]. For wastewater however, factors such as additional leachates, chlorine stability and ease of disposal should also be considered. These additional considerations along with discounting those with high non-specific adsorption tendencies eliminate the choice of many commonly used synthetic substrates. Many smart membranes have been developed as a grafted hydrogel to the surface of a synthetic material substrate. Grafting is a favoured process as it produces a deposited hydrogel with high functionality. However, it is limiting to commercialization since grafting methods such as ATRP and surface initiation plasma treatment can have combinations of long production times, high resource requirement or uses strong acids/bases [48-51].

1.3 Positive Thermo-Responsive Membranes

Stimuli-responsive membranes are an attractive technology as the stimuli can be non-intrusive to a process or have very specific sensitivity. As water temperature varies predictably in the environment and is an easily manipulated stimulus under controlled settings, membranes adapted from a thermo-responsive, water soluble polymer gel (hydrogel) are often chosen for smart membrane development. Thermo-responsive hydrogels undergo swell-collapse volume-phase transitions in response to heating and cooling. When deposited on the surfaces of porous membranes, hydrogels have been shown to reversibly fill and vacate (open and close) membrane pores as a gating mechanism as well as change surface characteristics [38, 40].

There are two main classifications of observed thermo-responsive behaviour in hydrogels, positive volume-phase transitions (PVT) and negative volume-phase transitions (NVT). Each behaviour type has a volume-phase transition temperature (VTT) dividing the conditions of swollen and collapsed volume-phases. A PVT hydrogel will swell upon heating, increasing its volume, and typically maintain a collapsed conformation at temperatures below its VTT. An NVT hydrogel will collapse upon heating, decreasing its volume, while maintaining a swollen conformation at temperatures below its VTT. The volume-phase transition is typically reversible but not in all cases and hysteresis is frequently experienced [52-56]. Chapter 2 details a review of prominent types of PVT polymers, their mechanisms of phase transition that could have application with smart membranes and gives reason to the choice of hydrogel coating used in this work.

1.4 Hypothesis

To improve a membrane's functionality in wastewater treatment application, it should have high hydraulic permeability so as not to require high driving pressures. Higher hydraulic permeability is usually only achievable through larger pore size so the membrane should have an increased surface functionality to make up for reduced size exclusion capability. The surface functionality should be specific enough to target oestrogens like 17β-estradiol but reject them easily in a regeneration cycle. The characteristics of oestrogen hormones that should be considered are their small size, low water solubility (hydrophobicity) and potential for hydrogen bonding due to unhindered hydroxyl groups [24, 25, 57]. E2 is specifically 272 Da, has a $\log K_{ow}$ of ~4 and has two hydroxyl groups (See Figure 1). Stimuli-responsive membranes can regenerate by reversibly changing surface functionality. The enacting stimulus must be able to function in aqueous conditions through large volumes of flow and not leave any potentially harmful residue. Recalling hydrogel stimuli mentioned earlier, chemical addition is typically undesirable in wastewater processes and would require environmental impact

study while applied electrical fields are dangerous around water processes. Temperature is an attribute that is relatively constant and it is also an easy variable to control in practical setups. There is opportunity for design of a smart membrane that can adsorb oestrogen contaminates at low wastewater temperatures specific to Canada and many other northern countries and then release the contaminants upon command at a higher temperature in a separate regeneration process. The membrane must therefore be able to change functionality above general wastewater temperatures but not at temperatures prohibitively high.

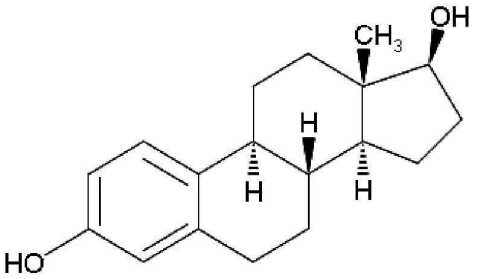

Figure 1: Molecular structure of 17β-estradiol.

Thesis Objectives

The objectives of this project were to; adapt a simple synthesis process for a thermo-responsive membrane on a paper substrate; characterize the temperature-permeation response of the membranes over various hydrogel coating compositions; and using 17β-estradiol as a model oestrogen, evaluate the adsorption capability of select coating compositions across various environmentally relevant temperatures.

1.5 Thesis Outline

This thesis describes the development of a smart membrane with a thermo-responsive gating mechanism capable of increased hydraulic permeability at low temperatures and reversible binding of estrogens from aqueous medium. The thermo-responsive membranes are composed of an Am-AA based hydrogel coated onto a Whatman filter paper substrate. Cellulose paper was chosen as it has been shown to have a low adsorption capacity for estrogens [24, 58]. Using a synthetic substrate would have introduced competing adsorption sites reducing the reversible binding capabilities of the hydrogel coating. Paper was also chosen for its natural source, making it an inexpensive and biodegradable material. The larger pore sizes of these depth filtration substrates give them a higher hydraulic productivity over non-porous or smaller pore membranes because of the lower pressures required to drive flow. The complex fibre network of cellulose filter paper generally has a large specific surface area that is beneficial for adsorptive retention [59]. An Am-AA based hydrogel was identified as the prime candidate for the

above intended use because of its reasonable temperature range of volume-phase transition (10^oC – 30^oC) and chemical stability. Using a coating procedure on a cellulose paper substrate, two applied hydrogel microstructures are investigated, a random copolymer and an interpenetrating network (IPN). Coating processes for thermo-responsive membranes are not common in literature so the functionality of any resulting membrane is unproven but a coating process has been shown to be feasible for fabrication of other stimuli-responsive membranes [37]. Where grafting techniques chemically bind individual chains of a hydrogel to a surface, coating relies on physical binding between a macromolecular hydrogel and substrate creating a composite material with stronger mechanical properties.

The synthesis and thermo-responsive permeability for several Am-AA based hydrogel coatings are characterized. Responsiveness of coatings varying crosslinker, monomer ratio and mass loading were examined. The temperature at which the hydrogen bonded Am-AA complex forms and dissociates is tuneable through incorporation of hydrophobic co-monomer. BMA is introduced to the Am-AA hydrogel coating both as random copolymer and as poly (Am-co-BMA) in the interpenetrating network (IPN) in a second series of membranes. This third monomer unit strengthens hydrophobic interactions which supplements the inter-chain bonds between Am and AA monomer units responsible for the thermo-responsive PVT and allows for the volume-phase transition temperature to be tuned. Inclusion of BMA should increase the VTT requiring a higher temperature to achieve the same swelling or collapse. While evaluating different coatings, the permeability response of the membranes was used as a measure of corresponding surface functionality.

Several membrane candidates were identified based on their permeability performance to be used to investigate reversible adsorption of hormones, using 17β-estradiol (E2) as a model oestrogen. It is hypothesized that adsorption of estradiol will occur primarily by hydrophobic aggregation or hydrogen bonding, both favoured by the membrane at low temperatures. The adsorption capacity was examined in a background electrolyte solution. Isolation of the type of adsorptive interaction most responsible for binding between the Am-AA smart membrane and E2 was attempted by exposure to a well-known hydrophobic hormone, human insulin. While insulin is a protein with a much larger size of 6 kDa, it is still small enough that size exclusion in these membranes should not be a significant factor.

Wet tensile strength tests are performed to investigate the mechanical strength of the coated membranes and environmental electron scanning microscopy was used to identify the dispersion of the coating onto the paper substrate. The membranes used for these experiments were selected based on their permeability function.

1.6 Chapter References

1. Fent, K., A.A. Weston, and D. Caminada, *Ecotoxicology of human pharmaceuticals.* Aquatic Toxicology, 2006. **76**(2): p. 122-159.
2. Kleywegt, S., et al., *Pharmaceuticals and Personal Care Products in the Canadian Environment: Research and Policy Directions*, in *NWRI Scientific Assessment Report Series* A.a.K.O. McLaughlin, Editor. 2007, Burlington. p. 53.
3. Servos, M., et al., *Endocrine Disrupting Substances*, in *NWRI Scientific Assessment Report Series*. 2001, National Water Research Institute: Burlington, ON. p. 17 - 21.
4. Heberer, T. and D. Feldmann, *Contribution of effluents from hospitals and private households to the total loads of diclofenac and carbamazepine in municipal sewage effluents – modeling versus measurements.* Journal of Hazardous Materials, 2005. **122**: p. 211.
5. Phillips, P.J., et al., *Pharmaceutical formulation facilities as sources of opioids and other pharmaceuticals to wastewater treatment plant effluents.* Environmental Science and Technology, 2010. **44**: p. 4910.
6. Phillips, P.J., et al., *A multi-disciplinary approach to the removal of emerging contaminants in municipal wastewater treatment plans in New York State, 2003-2004.* Clearwaters, 2008. **38**(3): p. 48.
7. Koh, Y.K.K., et al., *Treatment and Removal Strategies for Estrogens from Wastewater.* Environmental Technology, 2008. **29**: p. 245.
8. Nakada, N., et al., *Fate of oestrogenic compounds and identification of oestrogenicity in a wastewater treatment process.* Water Science & Technology, 2006. **53**(11): p. 51-63.
9. Servos, M.R., et al., *Distribution of estrogens, 17β-estradiol and estrone, in Canadian municipal wastewater treatment plants.* Science of The Total Environment, 2005. **336**(1–3): p. 155-170.
10. Arcand-Hoy, L.D., A.C. Nimrod, and W.H. Benson, *Endocrine-Modulating Substances in the Environment: Estrogenic Effects of Pharmaceutical Products.* International Journal of Toxicology, 1998. **17**(2): p. 139-158.
11. Fotsis, T., *The multicomponent analysis of estrogens in urine by ion exchange chromatography and GC-MS—II. Fractionation and quantitation of the main groups of estrogen conjugates.* Journal of Steroid Biochemistry, 1987. **28**(2): p. 215-226.

12. Christen, V., et al., *Highly active human pharmaceuticals in aquatic systems: A concept for their identification based on their mode of action.* Aquatic Toxicology, 2010. **96**(3): p. 167-181.
13. Turan, A., *Excretion of natural and synthetic estrogens and their metabolites: Occurrence and behaviour in water*, in *Endocrinally Active Chemicals in the Environment*, A. Gies, Editor. 1995, German Federal Environment Agency: Berlin. p. 15-50.
14. Kolpin, D.W., et al., *Pharmaceuticals, Hormones, and Other Organic Wastewater Contaminants in U.S. Streams, 1999−2000: A National Reconnaissance.* Environmental Science & Technology, 2002. **36**(6): p. 1202-1211.
15. Ternes, T.A., et al., *Behavior and occurrence of estrogens in municipal sewage treatment plants: Investigations in Germany, Canada and Brazil.* Science of the Total Environment, 1999. **225**: p. 81.
16. GWRC, *Endocrine Disrupting Compounds: Occurrence of EDC in Water Systems*. 2003, London: Global Water Research Foundation.
17. GWRC, *Pharmaceuticals and Personal Care Products in the Water Cycle*. 2004, London: Global Water Research Foundation.
18. NRC, U.S., *Hormonally active agents in the environment*. 1999, Washington, DC: National Academy Press.
19. Mons, M., *Samenvatting informatie geneesmiddelen*, in *BTO 2004.004*. 2004, Kiwa Water Research: Nieuwegein. p. 45.
20. Lange, A., et al., *Altered sexual development in roach (Rutilus rutilus) exposed to environmental concentrations of the pharmaceutical 17alpha-ethinylestradiol and associated expression dynamics of aromatases and estrogen receptors.* Toxicology Science, 2008. **106**: p. 113.
21. Lange, A., et al., *Sexual reprogramming and estrogenic sensitization in wild fish exposed to ethinylestradiol.* Environmental Science Technology, 2009. **43**: p. 1219.
22. Routledge, E.J., et al., *Identification of Estrogenic Chemicals in STW Effluent. 2. In Vivo Responses in Trout and Roach.* Environmental Science & Technology, 1998. **32**(11): p. 1559-1565.
23. Schäfer, A.I. and T.D. Waite. *Removal of endocrine disrupters in advanced treatment - the Australian approach*. in *IWA World Water Congress, Workshop Endocrine Disruptors*. 2002. Melbourne, Australia: IWA Specialist Group on assessment and control of hazardous substances in water (ACHSW).

24. Han, J., W. Qiu, and W. Gao, *Adsorption of estrone in microfiltration membrane filters.* Chemical Engineering Journal, 2010. **165**(3): p. 819-826.
25. Nghiem, L.D., A.I. Schäfer, and M. Elimelech, *Removal of Natural Hormones by Nanofiltration Membranes: Measurement, Modeling, and Mechanisms.* Environmental Science & Technology, 2004. **38**(6): p. 1888-1896.
26. Nghiem, L.D., A.I. Schäfer, and T.D. Waite, *Adsorptive interactions between membranes and trace contaminants.* Desalination, 2002. **147**(1–3): p. 269-274.
27. Schäfer, A.I., L.D. Nghiem, and T.D. Waite, *Removal of the Natural Hormone Estrone from Aqueous Solutions Using Nanofiltration and Reverse Osmosis.* Environmental Science & Technology, 2003. **37**(1): p. 182-188.
28. Yoon, Y., et al., *Nanofiltration and ultrafiltration of endocrine disrupting compounds, pharmaceuticals and personal care products.* Journal of Membrane Science, 2006. **270**(1–2): p. 88-100.
29. Yu, Z., et al., *Sorption of steroid estrogens to soils and sediments.* Environmental Toxicology and Chemistry, 2004. **23**(3): p. 531-539.
30. Nghiem, L.D., et al., *Estrogenic hormone removal from wastewater using NF/RO membranes.* Journal of Membrane Science, 2004. **242**(1–2): p. 37-45.
31. Zhang, Y., et al., *Removal of bisphenol A by a nanofiltration membrane in view of drinking water production.* Water Research, 2006. **40**(20): p. 3793-3799.
32. Adams, C., et al., *Removal of Antibiotics from Surface and Distilled Water in Conventional Water Treatment Processes.* Journal of Environmental Engineering, 2002. **128**(3): p. 253.
33. Chu, L., R. Xie, and X. Ju, *Stimuli-responsive Membranes: Smart Tools for Controllable Mass-transfer and Separation Processes.* Chinese Journal of Chemical Engineering, 2011. **19**(6): p. 891-903.
34. Ulbricht, M., *Advanced functional polymer membranes.* Polymer, 2006. **47**(7): p. 2217-2262.
35. Jeon, G., et al., *Electrically Actuatable Smart Nanoporous Membrane for Pulsatile Drug Release.* Nano Letters, 2011. **11**(3): p. 1284-1288.
36. Chen, X.N., et al., *Surfaces Modified by Amphiphilic Copolymer: Preparation and Application.* Advanced Materials Research, 2008. **47-50**: p. 1311-1314.
37. Mah, K.Z. and R. Ghosh, *Paper-based composite lyotropic salt-responsive membranes for chromatographic separation of proteins.* Journal of Membrane Science, 2010. **360**(1-2): p. 149-154.

38. Chu, L.-Y., et al., *Negatively Thermoresponsive Membranes with Functional Gates Driven by Zipper-Type Hydrogen-Bonding Interactions.* Angewandte Chemie International Edition, 2005. **44**(14): p. 2124-2127.

39. Liang, L., et al., *Temperature-sensitive membranes prepared by UV photopolymerization of N-isopropylacrylamide on a surface of porous hydrophilic polypropylene membranes.* Journal of Membrane Science, 1999. **162**(1-2): p. 235-246.

40. Park, Y.S., Y. Ito, and Y. Imanishi, *Permeation Control through Porous Membranes Immobilized with Thermosensitive Polymer.* Langmuir, 1998. **14**(4): p. 910-914.

41. Kwon, I.C., Y.H. Bae, and S.W. Kim, *Electrically credible polymer gel for controlled release of drugs.* Nature, 1991. **354**(6351): p. 291-293.

42. Tanaka, T., et al., *Collapse of Gels in an Electric Field.* Science, 1982. **218**(4571): p. 467-469.

43. Briscoe, B., P. Luckham, and S. Zhu, *On the effects of water solvency towards non–ionic polymers.* Proceedings of the Royal Society of London. Series A: Mathematical, Physical and Engineering Sciences, 1999. **455**(1982): p. 737-756.

44. Tanaka, T., *Collapse of Gels and the Critical Endpoint.* Physical Review Letters, 1978. **40**(12): p. 820.

45. Yu, D., et al., *Paper-PEG-based membranes for hydrophobic interaction chromatography: Purification of monoclonal antibody.* Biotechnology and Bioengineering, 2008. **99**(6): p. 1434-1442.

46. Zhang, K. and X.Y. Wu, *Temperature and pH-responsive polymeric composite membranes for controlled delivery of proteins and peptides.* Biomaterials, 2004. **25**(22): p. 5281-5291.

47. Zhou, X., et al., *Investigation of pH sensitivity of poly(acrylic acid-co-acrylamide) hydrogel.* Polymer International, 2003. **52**(7): p. 1153-1157.

48. Kuroki, H., et al., *Biomolecule-Recognition Gating Membrane Using Biomolecular Cross-Linking and Polymer Phase Transition.* Analytical Chemistry, 2011. **83**(24): p. 9226-9229.

49. Zhao, Y.-H., K.-H. Wee, and R. Bai, *A Novel Electrolyte-Responsive Membrane with Tunable Permeation Selectivity for Protein Purification.* ACS Applied Materials & Interfaces, 2009. **2**(1): p. 203-211.

50. Chu, L.-Y., et al., *Thermoresponsive transport through porous membranes with grafted PNIPAM gates.* AIChE Journal, 2003. **49**(4): p. 896-909.

51. Rattan, S. and T. Sehgal, *Stimuli-responsive membranes through peroxidation radiation-induced grafting of 2-hydroxyethyl methacrylate (2-HEMA) onto isotactic polypropylene film (IPP).* Journal of Radioanalytical and Nuclear Chemistry, 2012. **293**(1): p. 107-118.

52. Azzaroni, O., A.A. Brown, and W.T.S. Huck, *UCST Wetting Transitions of Polyzwitterionic Brushes Driven by Self-Association.* Angewandte Chemie, 2006. **118**(11): p. 1802-1806.

53. Georgiev, G.S., Z.P. Mincheva, and V.T. Georgieva, *Temperature-sensitive polyzwitterionic gels.* Macromolecular Symposia, 2001. **164**(1): p. 301-312.

54. Katono, H., et al., *Thermo-responsive swelling and drug release switching of interpenetrating polymer networks composed of poly(acrylamide-co-butyl methacrylate) and poly (acrylic acid).* Journal of Controlled Release, 1991. **16**(1-2): p. 215-227.

55. Seuring, J. and S. Agarwal, *Non-Ionic Homo- and Copolymers with H-Donor and H-Acceptor Units with an UCST in Water.* Macromolecular Chemistry and Physics, 2010. **211**(19): p. 2109-2117.

56. Tanaka, T., et al., *Phase Transitions in Ionic Gels.* Physical Review Letters, 1980. **45**(20): p. 1636.

57. Shareef, A., et al., *Aqueous Solubilities of Estrone, 17β-Estradiol, 17α-Ethynylestradiol, and Bisphenol A.* Journal of Chemical & Engineering Data, 2006. **51**(3): p. 879-881.

58. Walker, C.W. and J.E. Watson, *Adsorption Of Estrogens On Laboratory Materials And Filters During Sample Preparation.* J. Environ. Qual., 2010. **39**(2): p. 744-748.

59. Weatherwax, R.C., *Transient pore structure of cellulosic materials.* Journal of Colloid and Interface Science, 1974. **49**(1): p. 40-47.

2. Positive Thermo-responsive Hydrogels for Application with Smart Membranes

Typical thermo-responsive membranes use a NVT hydrogel such as poly(N-isopropylacrylamide) (PNIPAm) since PVT behaviour in water is uncommon for polymer gels [1-4]. PNIPAm hydrogels assume a swollen state at cooler temperatures and collapse with heating [5, 6]. However, PNIPAm and other NVT gels do not provide the required function in cold water that has been determined for this project. This chapter examines the properties and uses of common PVT hydrogels. Thermo-responsive hydrogel networks rely on chemical bonds for structure and physical bonds in order to undergo volume-phase transition. Physical bonds that are formed or broken during a phase transition are a combined effect of cooperative polymer-polymer interactions and polymer-solvent interactions [39-41]. Phase transition is thusly an equilibrium between dissociative forces that move to swell the gel and associative forces that move to collapse the gel. In terms of polymer-polymer interactions, associative forces are hydrophobic interactions and van der Waals interactions while electrostatic interactions and hydrogen bonding may act as both associative and dissociative forces depending on the environmental conditions.

2.1 Polysulfobetaine Hydrogels

Polyzwitterion hydrogels refer specifically to electrolytic polymer gels that contain both positively and negatively charged pendant groups. Polybetaine hydrogels are those polyzwitterionic hydrogels where oppositely charged groups are on nonadjacent sites of the same monomer unit and the cation doesn't have an associated hydrogen (Figure 1). Polybetaine hydrogels are temperature responsive, a unique quality not typical of other polyzwitterions.

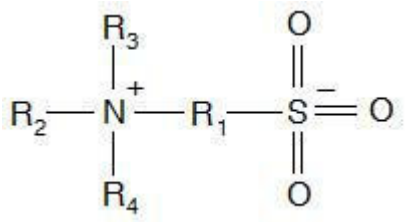

Figure 1: Sulfobetaine functional unit

Early workers were required to synthesize their own sulfobetaine monomers, limiting the amount of research done for solution behaviour. After polymerization, lengthy fractionation was also required to achieve adequately narrow polydispersity [7]. The commercial availability of sulfobetaine monomers enabled more research into solution

properties of single polymers and gels in solution. N-(2-methacryloyloxyethyl)-N,N-dimethyl-N-(3-sulfopropyl) ammonium betaine was one of the first such monomers, offered under the name SPE by Raschig GmbH [8]. Along with the other IUPAC names for the compound (CAS# monomer: 3637-26-1, polymer: 41488-70-4), this monomer has been called sulfobetaine methacrylate (SBMA), DMMAPS and MEDSAH by other workers [9-13]. It was noted by Soto and Galin that although polysulfobetaine solubility is good in protic solvents, solubility in water above 20°C was unusual and was reaffirmed later [14]. However it was also later found that solubility of polySPE in water was achieved at room temperature or upon heating. This signified that polySPE and possibly other polysulfobetaines have temperature dependent solution properties. Schulz was able to confirm this using cloud point titrations in both deionized water and salt water and map out the first full phase diagram for a sulfobetaine polymer in solution (Figure 2). The region above a coexistence curve represents one phase while the region below represents separation in two phases.

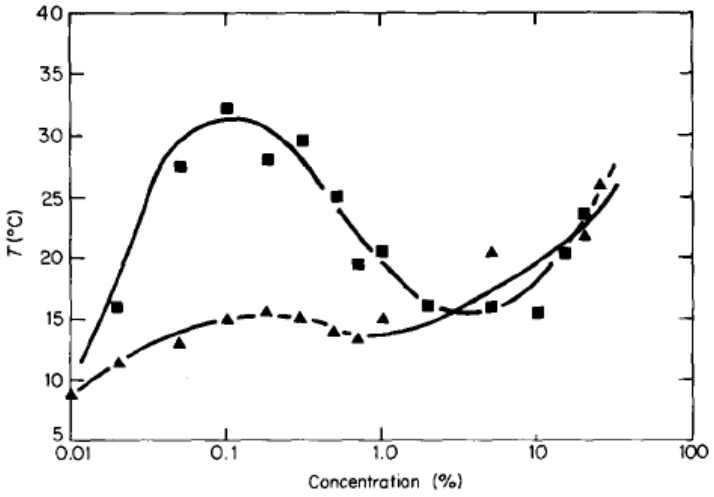

Figure 2: Effect of polymer concentration and salt on polySPE phase behaviour with respect to temperature. ■, Polymer $M_w = 4.35x10^5$; ▲, Salt water (0.51 M NaCl) [8]

Both lower and upper critical solution temperature behaviours were observed at 16°C and 33°C respectively. These behaviours correspond to NVT behaviour and PVT behaviour in hydrogels of polySPE. A claim that both behaviours should be possible for a single species is exemplified by this early work of Schulz. In agreement with Soto, it was also observed that salt solutions improve the solubility of polysulfobetaines. Thus when applied to temperature responsive solution properties, increasing salt concentrations decrease the PVT temperature. Schulz was able to identify that the solution properties of polySPE are due to intra-chain and intra-group associations. Intra-chain associations are hydrogen bonds and dipole attractions on the same chain and the intra-group association

is the ion pairing of the betaine. Strong intra-chain associations are what cause insolubility of the polymer. With the mention of inter-chain associations, the concept for PVT hydrogels was suggested but not discussed. Schulz was able to propose a model for the effect of salt on solution properties but was unable to account for the temperature responsiveness of the polySPE. Along with work on unperturbed dimension and θ-conditions, characterization of single polySPE chains in solution allow better understanding of the behaviour of the gels [15].

2.1.1 Polysulfobetaine Smart Membranes

A study of polySPE chains grafted to a surface, by surface initiated atom-transfer radical polymerization, gives great insight into the mechanics of a hydrogel with PVT properties [9]. Azzaroni exhibits two main cases in this research: a surface with low molecular weight (short) chains; and a surface with high molecular weight (long) chains. The two cases are comparable to gels with high and low degrees of crosslinking respectively. Low molecular weight chains represent short polymer sections between crosslink nodes while high molecular weight chains are similar to long polymer sections between crosslink nodes. Azzaroni expands upon the description given by Schulz for the forces behind PVT behaviour in polybetaines. He invokes discussion of the dielectric properties of water, solvation effects and excluded volume effects from hydration of the charged sites in breaking chain associations for gel swelling. The energy of the electrostatic forces must exceed the energy required for dehydration of the charged sites in order to form high degrees of inter and intra-chain associations. The degree of chain association was measured by water contact angle in this study and qualified in terms of hydrophobicity and hydrophilicity of the hydrogel surfaces. Azzaroni claims that in the case of short polymer chains, there is no chain association as the density of electrostatic interactions is too low, allowing complete hydration. Conversely, long polySPE chains present a high number of charged sites increasing the probability of electrostatic interaction and chain association, hindering hydration. The long grafted chains were poorly soluble in water at 22^{o}C, however, upon heating to 52^{o}C the gel coating shifted from a hydrophobic surface to a hydrophilic one. The shift was found to be reversible and the polySPE coatings maintained a stable composition for several months, able to undergo thermal cycling with similar results. Although this work is comparable to a true gel, it doesn't clearly qualitatively examine the equilibrium of interactions as the polybetaine is heated through its VTT nor does it present the extent of hydration quantified by the volume increase of the polymer network.

The work done by Azzaroni borrows the model of chain and group associations from research by Georgiev, who presented one of the first direct investigations of a polySPE hydrogel as it undergoes positive volume-phase transition [13]. Georgiev describes the

reversible swelling of the hydrogel as an equilibrium between inter and intra associations further developing the theory of Schulz and providing a basis for Azzaroni. The associations are described as intragroup ion pairs and entropy driven zwitterionic clusters (See Figure 3).

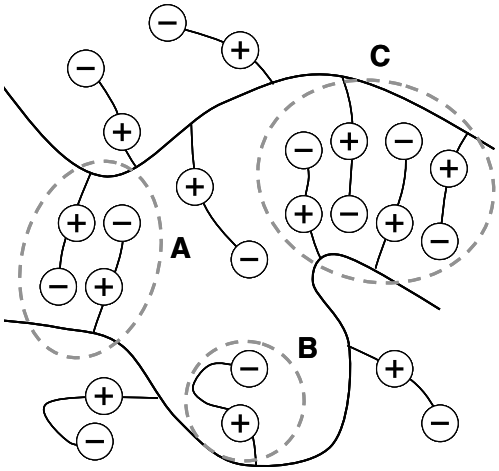

Figure 3: Short zwitterionic cluster (A), intragroup ion pair (B), long zwitterionic cluster (C), nucleated from a short cluster with entropy driven propagation outwards. Figure adopted from [13].

Georgiev is able to describe the shift of the equilibrium of the chain associations during the volume-phase transition. At low temperatures, zwitterionic clusters form as the enthalpy of the water decreases, making dehydration of the charged sites easier. The entropy of the solution also decreases, promoting higher order and a collapsed gel conformation. At high temperatures, increasing entropy and hydration energy favours ionic pairs allowing osmotic pressures to swell the gel. Dehydration of the charged sites is not mentioned by Georgiev as a factor in the volume transition of the hydrogel. The involvement of a dehydration activation energy is explored by Kamenova *et al.* [16], extending the model to include solvation factors in consolidation with the model of Azzaroni. This work assumes the model of associations established by Georgiev and uses an 'isoconversional method of thermogravimetric analysis' to approximate the activation energy of dehydration for the gels [17]. While attempting to correlate the results of the analysis on the dehydration activation energy to the equilibrium swelling ratio of the gels, the data and results are poorly presented restricting the usefulness of the work by Kamenova *et al.* to affirming the theory of Georgiev. Missing from all three works was whether any pendant chains remain unpaired as the charged sites are solvated by the water.

The discussion above on the effect of polymer segment length that was extrapolated from the grafted polySPE chains of Azzaroni is also addressed, confirming the contentions

presented. Hydrogels synthesized with low amounts of crosslinker provide long polymer segments between covalent nodes. It is observed that this leads to the abrupt positive change in swelling ratio observed across the VTT. This transition in swelling ratio becomes smoother and then disappears altogether at higher incorporation of crosslinker in the hydrogel. Additionally hysteresis is experienced upon cooling which is typical of dipole interactions seen in proteins undergoing coil-globule transition. These observations are used by Georgiev to infer that dipole-dipole associations as well as electrostatic interactions between ionic groups account for the large volume phase transition in the polybetaine hydrogels.

The progression of research with thermo-responsive polysulfobetaines has continued towards characterization and optimization of gel properties. Ethylene glycol dimethacrylate (EDMA) and N,N'-methylene bisacrylamide (MBAm) are typical crosslinkers when synthesizing polysulfobetaine gels. Attempts to optimize the hydrogel properties have used other crosslinking agents, with similar structure to SPE monomer, to improve the mechanical properties of polySPE gels [18]. This work shows that the concentration of crosslinker used in the synthesis of the hydrogel is more important for solution behaviour than selection of crosslinker. However, it is shown that different crosslink distances due to linker selection will have an impact of mechanical properties such as Young's modulus. Polysulfobetaines have also gained much interest as a biocompatible material with high protein fouling resistance[10]. Copolymerizations with other biocompatible thermo-responsive polymers have formed temperature triggered cell-detachment surfaces [19].

2.2 Acrylamide Based Hydrogels

Another significant class of PVT hydrogel is that of acrylamide (Am) based hydrogels. Many thermo-responsive hydrogels are Am-based as seen by work with PNIPAm and work on polysulfobetaines with an Am backbone [13, 20]. As will be shown, this class of hydrogel is dominated by hydrogen bonding. However, it is not as dominating as the electrostatic forces in the polysulfobetaine gels. Dipole interactions, electrostatic interactions and hydrophobic interactions play a larger part in balancing the forces of phase-transition for Am-based hydrogels. These gels are water soluble above $0^{o}C$ and able to swell several times their dry-weight to an extent highly dependant on their synthesis methods [21-24]. Although Am itself can be polymerized to form hydrogels, they do not undergo volume-phase transition. To form PVT hydrogels, Am is typically combined with acrylic acid (AA) either as a random copolymer or as an interpenetrating network of the homopolymers. The homopolymers of Am and AA in separate solutions behave like polymers in good solvent with near constant solubility upon heating while a mixture of the two in solution behaves like a polymer in poor solvent with improving

solubility upon heating [25]. It is known that hydrogen bonded complexes are formed between the two monomers and that these complexes break down upon heating [26, 27].

2.2.1 Interacting Forces

Although volume-phase transition had been shown for Am and AA polymer gels, complexation of the polymers by hydrogen bonding between the amide and carboxyl functional groups was first shown by Klenina [25]. Earlier work had examined interactions between the functional groups of Am and AA in acidic aqueous conditions [28, 29]. It was believed that the inclusion of AA accounted for ionization of the gel network and was responsible for discontinuous volume phase transition. However it was undetermined as to whether complexation occurred when AA was not ionized. Stable complexes between polyacrylamide (PAm) and polyacrylic acid (PAA) in solution were developed without dissociating the carboxyl groups. In hydrogel structure, the hydrogen bonding forms a ladder structure between polymer segments (Figure 4). The ladder structure is formed and broken by a "zipping" action nucleated from an individual hydrogen bond similar to the long zwitterionic clusters of the polysulfobetaine gels. Dissolution of the structure occurs upon heating and hydration forces are generated as hydrogen bonds are broken by thermal energy. The hydration forces break adjacent hydrogen bonds resulting in rapid dissolution as there are now two functional destructive forces. Similarly, upon cooling, a polymer-polymer hydrogen bonded structure is favoured as thermal energy decreases and is aided in forming bonds by propagating dehydration between adjacent side groups.

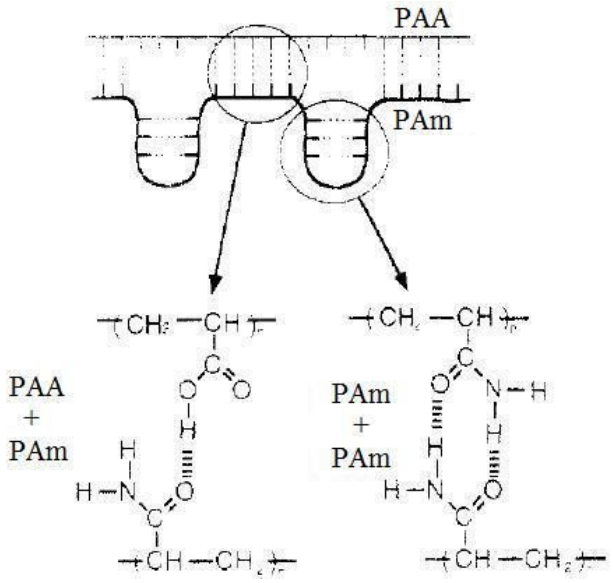

Figure 4: Competing hydrogen bond complexations in PAm and PAA hydrogels. Adapted with permission from [30]. Copyright 1994 American Chemical Society.

Dipole-dipole interactions between the amide groups present another strong influence over the volume-phase transitions. Water solubility of PAm is primarily controlled by the dipole interactions of the amide groups. In the homopolymer, it is expected that the energy produced by the amide dipole interactions is larger than that provided by solvent interactions and other solute interactions [31]. In the Am-AA gel network, hydrogen bonding becomes dominating, weakening the effect of the dipole interactions but not making them negligible. The amide dipoles may be affected by temperature just as the hydrogen bonds are. External stimuli can change the strength and alignment of the dipoles modifying the solution properties [32]. For Am-AA based hydrogels, there are two main competing intermolecular complexation mechanisms. Am can form complexes with itself, the discussion to whether this is due to hydrogen bonding or dipole interactions is ongoing, meaning that complete equimolar complexation with AA shouldn't possible as seen in Figure 4 [30].

Confirmation of hydrogen bonding in Am-AA based hydrogels is often provided using urea [20, 33], a known hydrogen bond and hydrophobic interaction disrupting analyte [34]. One worker reported complete dissolution of Am-AA complexes at 10 wt% urea in water as confirmed by light transmittance [35]. The effectiveness of urea does not clearly identify hydrogen bonding as the sole force causing dissolution. Hydrophobic interactions are enhanced at higher temperature and are a strong "attractive" force significant in negative volume-phase transitions. However, considering that a PVT hydrogel swells upon heating as well as with the addition of aqueous urea at low temperatures suggests that Am-AA based hydrogel networks experience negligible associative hydrophobic interactions. In addition to work with urea, varying the Am-AA monomer ratio can show that the hydrogen bond between amide and carboxyl functional groups is essential to positive volume-phase transition. Both PAm and PAA homopolymers show negligible volume change with temperature change in pure water [32, 36, 37]. It has been shown that in a gel network, the monomer ratio (Am:AA) must be between 1:9 and 8:2 for any volume phase transition to occur [35].

The swelling and collapse of a covalently crosslinked Am-AA based hydrogel is reversible and appears complete under light transmittance observation [35], however when viewed by mass or volume, reversibility is not complete with the absolute swelling volume becoming larger after each temperature cycle. Along with this, structure formation is kinetically slower than dissolution and hysteresis is often observed between heating and cooling cycles (Figure 5) [30, 32, 34, 35]. Both these effects have similar root causes. The typically high swelling ratios of Am-AA based hydrogels above their VTT impose great distances between polymer chains. These large interstitial spaces allow reduction in chain entanglement through the swelling and collapsing cycles, and, the polymer complexes formed below the VTT are not reformed as they once were, their

conformation changed as some chain segments may not reform complex at all [38]. Other aspects to consider, which will be discussed in following sections, are ionic dissociation of carboxyl groups and hydrophobic composition of the polymer chains.

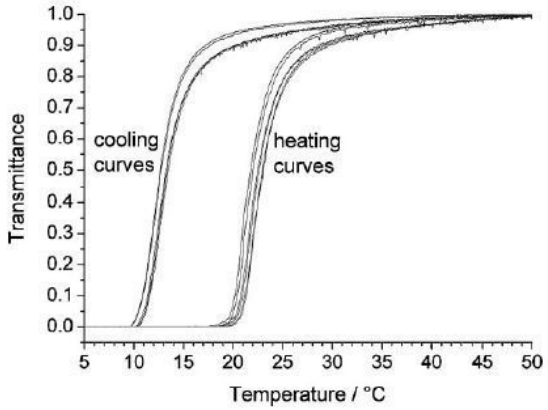

Figure 5: Hysteresis as observed by light transmittance characteristic of many Am-AA based hydrogels [39].

Stabilizing the polymer complex of PVT hydrogels has become a great topic of research as workers attempt to optimize the gel's responsive qualities. There are several strategies to do so: Increasing the amide density by using monomers with pendant groups with multiple amide functionality [40]; Increasing the hydrophobic content by copolymerization with a hydrophobic monomer [31, 35, 41, 42]; Suppress amide-amide interactions to promote more efficient amide-carboxyl complex formation [30, 43].

2.2.2 Hydrogel Synthesis

There are different volume-phase transition profiles that are attainable dependent on the microstructure of the Am-AA based hydrogel. The two most common structures are a random copolymer gel as well as an interpenetrating polymer network (IPN). The copolymers are typically prepared in a single polymerization step while the IPNs are prepared by sequential polymerization with the PAm network prepared first and the PAA network polymerized second. Workers have found that the random copolymerized hydrogels undergo smooth continuous volume transition through temperature change. The same workers have discovered IPNs to exhibit an abrupt volume change as the VTT of the hydrogel is attained. This abrupt change is often described as a discontinuous or discrete transition profile. It has been asserted that both the continuous and discrete Am-AA hydrogel transition behaviours are reversible in the sense described above [29, 38, 41].

There are common methods and recipes for synthesis of Am-AA based hydrogels. N'-methylene bisacrylamide is a double functional amide monomer that is frequently used as a crosslinking agent for these gels due to its similar structure (Figure 6).

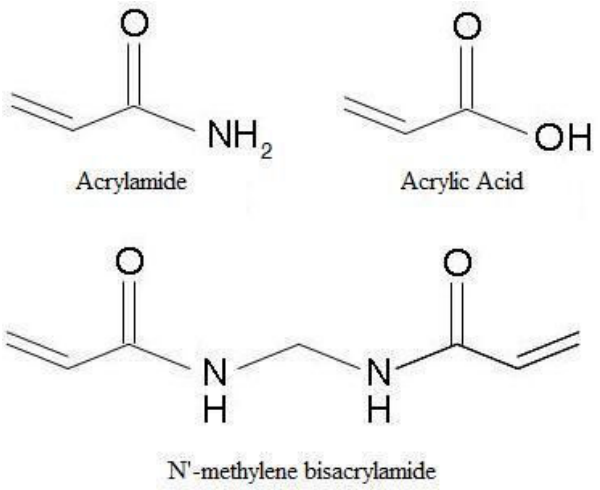

Figure 6: Chemical similarities between acrylamide, acrylic acid and N'-methylene bisacrylamide.

Initiation for Am-AA based hydrogels is typically by free radical initiation. Thermally activated persulfate initiators like ammonium persulfate (AP) or potassium persulfate are often combined with an accelerator like tetraethylmethylenediamine (TEMED) to reduce the temperature of initiation. The crosslinker and choice of initiator are also common to other thermo-responsive hydrogels using N-alkyl substituted amide monomers [20]. Additional methods of initiation that have been used are irradiation and plasma treatment (see Table 1) as well as reversible addition-fragmentation chain transfer (RAFT) [44]. Hydrogel polymerization is usually carried out in glass pipettes, between glass plates with spacers or in glass dishes. Earlier it was mentioned that a range of monomer ratios were acceptable for a Am-AA hydrogel to posses PVT behaviour, however, as shown in single polymer chain solutions of PAm and PAA, precipitates that form below the VTT have a stoichiometric ratio of 1:1 by refractive index analysis [25]. Results of this nature lead researchers who are developing hydrogels for functional application to design gels to have a 1:1 Am-AA monomer ratio in the final gel. Consistent of all workers, Am quantity is used to determine the amount of AA to satisfy the ratio.

Tanaka was one of the first researchers to work with PVT hydrogels. Initial work solely observed PAm gels and found discrete swelling behaviour with respect to temperature in partial organic solvent [36]. As asserted above, PAm does not exhibit temperature responsiveness in aqueous solvent. Work to discover conditions that would allow PAm hydrogels a volume phase transition in water was extensive, even leading Tanaka to

develop the spinodal curve for PAm [45]. It was discovered serendipitously that the gels needed to cure or "ionize" in order for PVT behaviour to occur without partial organic solvent [37]. Older gels underwent volume collapse upon cooling while more freshly synthesized gels did not. Tanaka's "ionization" turned out to be inclusion of carboxyl groups in the gel network [29]. This was possible by either hydrolysis of the amide groups or incorporation of AA as a co-monomer. In his early works, positive volume-phase transition was induced by partial hydrolysis of the amide groups in a basic reaction medium (pH 12). It was discovered that while only a small fraction of AA units were necessary for volume-phase transition to occur in water, increasing fractions promoted discrete volume phase transitions. Tanaka surmised that the swelling transitions in aqueous media could be accounted for by osmotic pressure driven by dissociation of hydrogen ions from the carboxyl groups, leading to his use of Flory-Higgins solution theory [36, 37].

Table 1: Various recipes for Am-AA based hydrogels

Am	AA	Crosslinker	Initiator	Type	Source
5 g	---	MBAm	AP & TEMED	Homopolymer	[29, 36, 37]
5g	5g	MBAm	AP & TEMED	Sequential IPN	[33]
7.2 g	7.3 g	MBAm	AP	Sequential IPN	[30]
15 – 30 mol%	Various molar ratios	---	^{60}Co-γ irradiation	Random copolymer	[46]
1:1 molar ratio		MBAm	Potassium peroxodisulfate	Random copolymer	[47]
1.775 g	1.800 g	MBAm	α-Ketoglutaric acid	Random copolymer	[48]
1-3 wt%	0.2-2 wt%	MBAm	Plasma treatment, potassium persulfate	Sequential IPN	[49]

The results of Tanaka showing discrete swelling transition was primarily based on solvent composition, never truly able to model a direct correlation between temperature and volume-phase transition in water, instead deriving a "reduced temperature" from the Flory-Higgins' osmotic pressure formula. The failure to model a direct relationship between temperature and hydrogel volume phase transition made Tanaka's work difficult to test. First works developing Am-AA hydrogels discovered this as only smooth, continuous swelling profiles were observed for random copolymer gels while the IPNs displayed an abrupt discrete transition [38, 41]. It was determined that rapid polymer complex formation and dissolution was responsible for the sharp volume transition observed for the IPN gels. The dull swelling of the copolymer was assumed to be due to

structural discontinuities causing isolation of any Am-AA complexes that did form. As discussed above, complex formation and dissolution are both nucleated at specific sites and then aided in outward propagation by hydration forces. The random ordering of amide and carboxyl groups as well as the isolated Am-AA complexes in the copolymer gel prevents large range influence of nucleation sites. The homopolymer chain segments between crosslink nodes in the IPN promote more efficient complex formation and therefore dissolution. Equimolar composition of the IPN was perpetrated as the optimum condition for complete complexation of the hydrogel below the VTT. This was not confirmed by the researchers as it was assumed that there was no concentration gradient through the initial PAm gel as it swelled with AA monomer solution prior to the secondary polymerization.

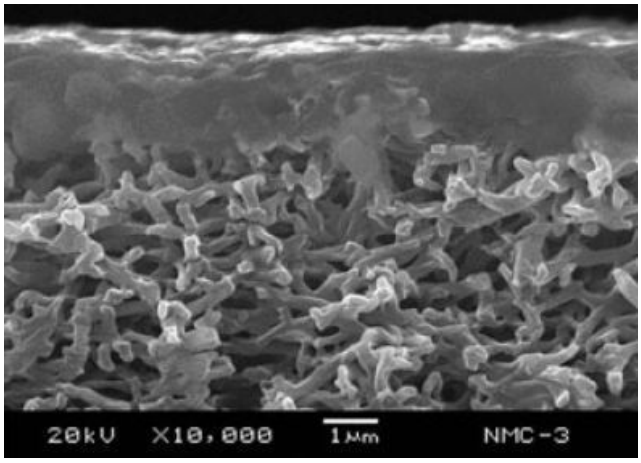

Figure 7: Scanning electron microscope image of nylon-6 membrane after sequential polymerization of a Am-AA IPN [49].

Application of Am-AA IPNs is well exemplified by work done grafting the hydrogel onto a porous nylon-6 substrate to create function gates to control permeability [49]. Consistent with the sequential polymerization method, PAm gels were surface initiated by plasma treatment to graft the initial gel onto the inside of the substrate pores. The initial gel was then swelled in an aqueous AA, MBAm, and potassium persulfate mixture before the secondary gel was polymerized. The functional gates showed that water permeability of the nylon substrate could be increased at temperatures below the VTT as the hydrogel collapsed, opening the pores. The pores would close above the VTT as the hydrogel gates swelled. Scanning electron microscopy and x-ray photoelectron spectroscopy were used to verify the structure of the membrane and the synthesis of the IPN. It was found that although the entire membrane was soaked in the secondary gel reaction mixture, it was only retained in the PAm gel (Figure 7). The PVT behaviour of the IPN hydrogel gates

was observed to be reversible through several temperature cycles varying between 10°C and 40°C.

2.2.3 Introducing Hydrophobic Content

Hydrophobic co-monomer is incorporated either by randomly copolymerization along with the Am and AA monomers or by randomly copolymerization with Am into the initial gel of a sequential IPN. Hydrophobic functional groups affect the complexation of amide and carboxyl groups in two main ways. Firstly, the hydrophobic groups increase the density of hydrophobic interactions. Hydrophobic interactions are strengthened at higher temperatures, so as hydrogen bonds break upon heating, hydrophobic interactions become more significant. Secondly, the hydrophobic functional groups in the polymer segments reduce the proximity of the amide groups from each other as well as from carboxyl groups, increasing the significance of polymer-solvent hydrogen bonding. This enhances the overall water solubility of the polymer as inter-chain associations are reduced [31]. Table 2 shows the quantities of hydrophobic monomer used in several studies. Butyl methacrylate (BMA) is the most commonly used hydrophobic monomer.

Table 2: Various recipes for hydrogels incorporating hydrophobic monomer

Am	AA	Hydrophobic monomer	Initiator	Type	Source
3.80 g	3.85 g	BMA (0.2 g)	t-Butyl peroctanoate, AP	Sequential IPN	[38, 41]†
3.60 g	3.65 g	BMA (0.4 g)	AP	Random copolymer	
6.408 g	6.497 g	BMA (1.584 g)	AP	Sequential IPN	[30]
1.6 g	1.6 ml	BMA (1.6 ml)	AP	Random copolymer	[42]
1:1 molar ratio		Octylphenol polyoxylethylene ether (3 mol%)	Potassium persulfate	Random copolymer	[35]

† various monomer ratios and quantities were used in these studies.

It is the consensus of these workers that incorporating a hydrophobic monomer into the hydrogel network increases the stability of the associative forces preventing swelling. This stability is observed as an increase in the VTT for the complex. Further increases in hydrophobic content raises the VTT even more, however a critical point where the gel is no longer water soluble is not reached by any worker [30, 38, 41, 42]. As well, at high BMA loadings, the volume-phase transition ceased to be significant and was only attainable at temperatures above 60°C. One researcher suggested that the reduced

swelling of hydrogels with higher BMA content was because BMA decreased the porosity of the gel network, however this explanation was flawed due to the setup of the experiment [42]. This presented model failed to discuss the effect of higher polymer loading causing a denser network.

The work using octylphenyl polyoxyethylene ether (OP7-AC) as the hydrophobic monomer was interesting as a crosslinking agent was not used [35]. First it should be noted that the monomer needed to be modified by adding an acryloyl chloride group in order for it to be polymerized into the Am chain. The synthesized hydrogel incorporating OP7-AC was crosslinked by interconnecting micelles of the OP7-AC pendant chains stabilized by sodium dodecyl sulphate (SDS) (Figure 8). These micelles acted as the physical crosslinks.

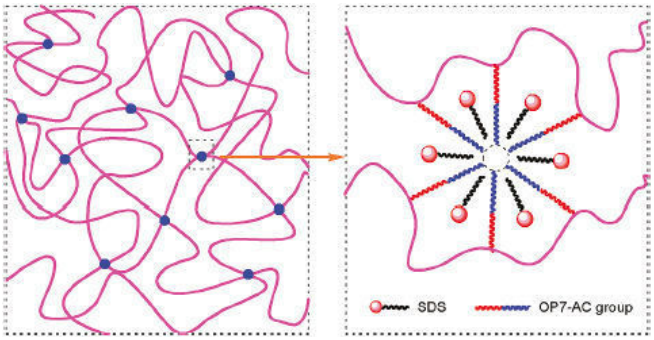

Figure 8: Micellular crosslinks of OP7-AC and SDS. Reprinted with permission from [35]. Copyright 2010 American Chemical Society.

The effects of different concentrations of SDS and OP7-AC were investigated. SDS, as the micelle stabilizing molecule, becomes more effective at higher concentrations raising the VTT with increasing concentration. Increasing OP7-AC content in the hydrogel initially decreased the VTT sharply to a minimum of ~12^{o}C at 1.5 wt% of the monomer as the hydrophobic group disrupted amide-amide interactions and competed with the carboxyl groups for hydrogen bonding with the amide groups. Hydrophobic interactions became more dominant at higher OP7-AC inclusion, gradually increasing the VTT. In the earlier work of Katono *et al.* it had been observed that inclusion of BMA in the hydrogel composition improved the mechanical strength of the gel and although this was a qualitative observation, suggested this to be typical effect for the inclusion of any hydrophobic monomer [38]. This was investigated for hydrogels containing OP7-AC as well. Stress-strain curves were prepared for several hydrogel recipes showing higher Am content promoted better stress properties while higher AA content promoted better elongation properties. Gels incorporating OP7-AC were not compared to similar gels making the results quantitatively inconclusive as to whether the mechanical properties were indeed improved.

2.2.4 Stabilizing Am-AA Complexation

The suppression of amide-amide interactions is one of the effects of incorporating a hydrophobic co-monomer into the hydrogel network. However copolymerization of the hydrophobic monomer doesn't always lead to more efficient hydrogen bonding between the amide and carboxyl groups as was seen with OP7-AC which had its own competing hydrogen bonding. There is another way to include hydrophobic functional groups which disrupt the dipole interactions between amide groups but do not hydrogen bond or create a steric hindrance which disables volume-phase transition. Substituting alkyl groups on the nitrogen of the amide introduces a hydrophobic property without additional monomers. There is a balance however between the size of the substituted alkyl group and the strength of the amide-carboxyl hydrogen bond. NIPAm is one such N-substituted Am where the isopropyl group fully disrupts the interchain hydrogen bonding and hydrophobic interactions become dominant, promoting NVT behaviour. N,N'-dimethylacryamide (DMAm) is a N-substituted Am that has been used with AA in IPN hydrogels to improve the amide-carboxyl group hydrogen bonding efficiency [30]. Like other IPNs, the DMAm monomer is copolymerized with Am to form the initial gel for a sequential IPN synthesis. MBAm and AP are used, respectively, as the crosslinking agent and initiator. Concentrations of DMAm used in the synthesis of the initial poly(DMAm-co-Am) gel varied between 0 mol% and 27 mol%. Similar to the other hydrogels incorporating a hydrophobic co-monomer, increasing DMAm content in the composition of poly(DMAm-co-Am)/PAA IPNs caused the VTT to rise. This was confirmed by UV-transmittance, the VTT rose from 25^{o}C at 0 mol% DMAm to 40^{o}C at 20 mol% (Figure 9A).

As briefly discussed, PAm can form hydrogen bonded complexes with itself which means that it shouldn't be able to form a completely equimolar complex with PAA. PAm is a hydrogen donor and acceptor. PAA is a hydrogen donor. PDMAm is a hydrogen acceptor. This work argues that DMAm cannot form hydrogen bonded complexes with itself which allows equimolar complex formation with PAA (See Figure 9B). This assertion by Aoki *et al.* is not wholly correct. If PAm can form hydrogen bonds with itself as both a donor and acceptor, it should be able to form hydrogen bonds with PDMAm where the Am unit acts a donor. Instead, it is possible that the Am self associations due to dipole-dipole interaction of the amide are a stronger associative force than the amide-amide hydrogen bonding. Am dipole-dipole interactions are disrupted by the non-polar N-alkyl substituted group. The substituted alkyl groups on the pendant chains of PDMAm prevent the amide from undergoing dipole-dipole interactions hence it cannot associate with PAm.

A) 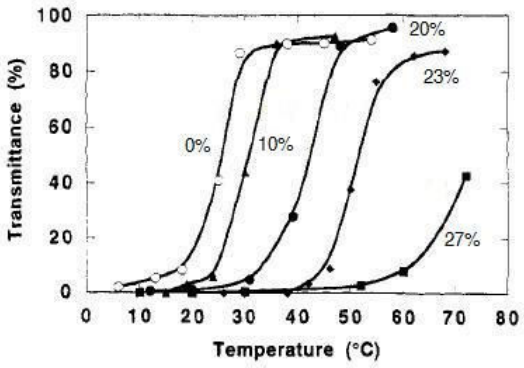

B) 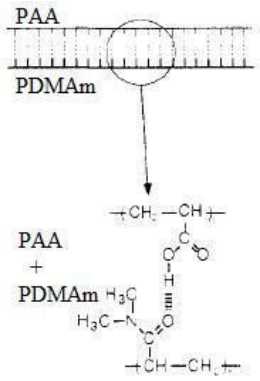

Figure 9: Effect of DMAm content on poly(DMAm-co-Am)/PAA IPN (A). Percentages are by mol. Complexation of PDAm with PAA (B). Adapted with permission from [30]. Copyright 1994 American Chemical Society.

DMAm promotes more efficient amide-carboxyl complexation in Am-AA based hydrogels only when incorporated as a comonomer with Am in the initial gel of an IPN. While PDMAm and PAA homopolymers can form strong complexes with each other in solution, poly(DMAm-co-AA) does not form a complex nor does PDMAm-graft-PAm [43]. The DMAm monomer unit has not been shown to impart temperature dependant solution properties, Am is still required.

2.3 Novel PVT Hydrogels

N-Acryloyl glycinamide (NAGA), or N-(carbamoylmethyl)prop-2-enamide (Figure 10), is a monomer compound whose homopolymer (PNAGA) is capable of forming a thermally reversible, non-covalently bonded gel network in water. This temperature dependant hydrogel was first observed and extensively studied by Haas et al. [50-55]. Since this first observation and study there have been very few works further investigating the characteristics and mechanisms of the complexation of NAGA as either homopolymer or co-monomer [56].

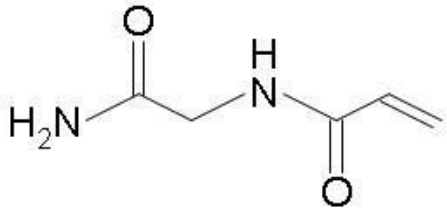

Figure 10: N-Acryloyl glycinamide

A renewed interest in 2007 [57] apparent in patent literature and again in 2010 [58] for the solution properties of single polymer chains and synthesis methods for PNAGA suggests that more investigations of the characteristics and properties of NAGA-based

gels may be expected in the future [39, 59, 60]. The only previous work to observe the PVT behaviour of NAGA-based gels was with IPNs by Sasase et al. [40]. Based on the observation of a VTT of 35^{o}C for hydrogen bonded complexes of PNAGA and PAA in solution, sequential IPNs were synthesized incorporating BMA. Poly (NAGA-co-BMA)/PAA IPNs were synthesized and showed increased swelling with heating. Similar to other gels, the swelling ratio decreased at higher BMA content. These IPNs were compared to poly(Am-co-BMA)/PAA IPNs. When NAGA was substituted for Am in the hydrogel, the extent of swelling was lesser and the VTT was higher. These results suggested that NAGA groups were capable of forming stronger hydrogen bonds than Am groups with AA groups.

The early works by Haas et al. did not actually determine volume-phase transition for PNAGA polymers. Thermo-reversible gelation driven by randomly distributed hydrogen bonding was all that was observed. PNAGA is one of the rare temperature responsive polymers where PVT behaviour was observed with the hydrogel prior to being characterized as single chains in solution. The more recent works are inspired by the work of Seuring *et al.* exhibiting the positive volume-phase transition of PNAGA in water [39]. The significant difference between a polymer solution in water undergoing thermo-gelation and the PVT behaviour of a hydrogel is phase separation. The novel aspect of PNAGA having a VTT in water is that it does so as a homopolymer and it is non-ionic. All the temperature responsive hydrogels that have been discussed so far are either ionic, which limits their functionality in physiological and environmental milieu, or multiple monomer specie networks. Similar to the polysulfobetaines, the pendant chains of PNAGA are capable of forming both inter and intra complexes without requirement of an additional hydrogen acceptor monomer species. The primary amide acts as the hydrogen donor and the carbonyl acts as the hydrogen acceptor. The VTT was determined to be ~22.5^{o}C upon heating and ~12.3^{o}C upon cooling by a turbidity photometer at 670 nm at a heating rate of 1 ^{o}C·min^{-1}. A later publication by Seuring *et al.* investigated why PVT behaviour for PNAGA had not been observed while it had been know to undergo thermo-reversible gelation for near half a century [60]. It was determined that any ionized groups in the polymer prevent phase separation, ionic groups can be introduced unintentionally by either “acrylate impurities in the monomer, hydrolysis of the polymer side chains, and/or usage of ionic initiators or chain transfer agents”. This work presents explanation for alternate synthesis attempts to polymerize PNAGA [59]. RAFT polymerization is attractive to many polymer scientists as is can be used to control the chain length of the polymers synthesized. It was observed that PNAGA synthesized in this method did not show a VTT in water but instead reflected the work of Haas et al. The PNAGA that did show a VTT in water was synthesized by free radical initiation from azo-bis-isobutyronitrile.

The work by Seuring *et al.* was extended to examine NAGA in copolymerization with N-acetyl acrylamide (NAcAm) [39], an hydrogen acceptor, to investigate the nature of the hydrogen bonds proliferated by NAGA. NAcAm was chosen as it is similar in structure to NAGA but the propanamide moiety of the secondary amine is substituted with an acetyl group. This structure difference, although showing both hydrogen donating and accepting functionalities, did not display VTT behaviour in water. Copolymers with a NAGA mol fraction of 0.645 or lower did not exhibit a VTT either, although at higher NAGA mol fractions in the copolymer, the transition of solution to gel became smoother, less abrupt. This shows that the inter and intra-chain associations of the NAGA pendant groups are stronger than the inter-chain associations with other species since VTT increases with higher NAGA content in the copolymer and the transition becomes slower.

Following the example of characterizing previously discovered polymers, Glatzel et al. [59], attempted RAFT polymerization of N-Acryloylasparaginamide (NAAm), a monomer unit again similar to NAGA but with two primary amides instead of one (

Figure 11).

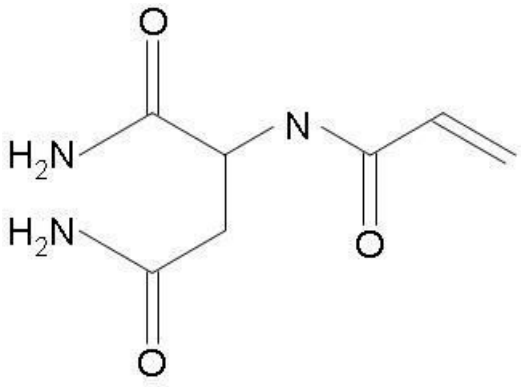

Figure 11: N-Acryloylasparaginamide

It was thought that by increasing the amide density, PVT polymers would result from a RAFT polymerization process. As well the water solubility of the NAAm monomer suggested strongly that the polymer would undergo volume-phase transition. Although this work was successful in presenting another novel characterization of a PVT polymer, it is a rudimentary first look into the volume-phase transition of poly (NAAm) in water. There is much work between this and development of a functional hydrogel for application to thermo-responsive membranes.

2.4 Review and Analysis

Polysulfobetaine and Am-AA hydrogels are the most established types of PVT hydrogel with previous application on thermo-responsive membranes. For polysulfobetaine

hydrogels, electrostatic interactions between the charged sites on the polymer side chains were the primary driving forces for volume-phase. But volume-phase transitions are an equilibrium between several forces. Although electrostatic forces driven by the ionic nature of the gel composition is the primary force, dipole-dipole interactions from the permanent, non-adjacent and opposite charges as well as minor hydrogen bonding play a part. Unmentioned are hydrophobic interactions between the long hydrocarbon-based polymer chains of the hydrogel. They were unaddressed by most workers as the hydrophobic interactions were not significant in the studied polysulfobetaines. Hydrogen bonding and dipole-dipole interactions between amide and carboxyl groups were the primary driving force for Am-AA hydrogels but it was also seen that the role of hydrophobic interactions could be manipulated through addition of hydrocarbon monomer or substituted moieties.

Control of the VTT is important for any application of thermo-responsive hydrogel. Creating membranes with temperature sensitive properties often requires that the coated or grafted hydrogel maintain a stable chemistry and physiology before and after the volume-phase transition. In application to wastewater removal of oestrogen, the PVT behaviour must be maintained through varying pH and tonicity. Disinfection chemicals used in many wastewater treatment processes could damage delicate chemistries. Polysulfobetaine hydrogels would be sensitive to pH and ionic content of the wastewater to an extent that functionality could be significantly diminished. Underdeveloped hydrogels do not have the strength of supporting synthesizing methods or response characterization to merit practical application for smart membranes. While the function of Am-AA membranes is affected by pH, it does not greatly alter the volume-phase transition within realistic environmental pH values. Also there is much evidence for the modification of Am-AA hydrogels to adapt not only their effective VTT but also their surface functionality and chemical stability. Along with the practical working VTT range of Am-AA based hydrogels, these are the reasons they were chosen for this project.

2.5 Chapter References

1. Ying, L., E.T. Kang, and K.G. Neoh, *Synthesis and Characterization of Poly(N-isopropylacrylamide)-graft-Poly(vinylidene fluoride) Copolymers and Temperature-Sensitive Membranes.* Langmuir, 2002. **18**(16): p. 6416-6423.
2. Liang, L., et al., *Temperature-sensitive membranes prepared by UV photopolymerization of N-isopropylacrylamide on a surface of porous hydrophilic polypropylene membranes.* Journal of Membrane Science, 1999. **162**(1-2): p. 235-246.
3. Chu, L.-Y., et al., *Thermoresponsive transport through porous membranes with grafted PNIPAM gates.* AIChE Journal, 2003. **49**(4): p. 896-909.

4. Yang, M., et al., *Thermo-Responsive Gating Characteristics of Poly(N-isopropylacrylamide)-Grafted Membranes.* Chemical Engineering & Technology, 2006. **29**(5): p. 631-636.
5. Heskins, M. and J.E. Guillet, *Solution Properties of Poly(N-isopropylacrylamide).* Journal of Macromolecular Science: Part A - Chemistry, 1968. **2**(8): p. 1441-1455.
6. Pelton, R., *Temperature-sensitive aqueous microgels.* Advances in Colloid and Interface Science, 2000. **85**(1): p. 1-33.
7. Soto, V.M.M. and J.C. Galin, *Poly(sulphopropylbetaines): 2. Dilute solution properties.* Polymer, 1984. **25**(2): p. 254-262.
8. Schulz, D.N., et al., *Phase behaviour and solution properties of sulphobetaine polymers.* Polymer, 1986. **27**(11): p. 1734-1742.
9. Azzaroni, O., A.A. Brown, and W.T.S. Huck, *UCST Wetting Transitions of Polyzwitterionic Brushes Driven by Self-Association.* Angewandte Chemie, 2006. **118**(11): p. 1802-1806.
10. Kuo, W.-H., et al. *Hemocompatibility on Poly(acrylic acid -co- sulfobetaine methacrylate) Copolymer Polyelectrolyte Multilayer Modified Surfaces*. in *The 13th Asia Pacific Confederation of Chemical Engineering Congress*. 2010. Taipei.
11. Weaver, J.V.M., S.P. Armes, and V. Bütün, *Synthesis and aqueous solution properties of a well-defined thermo-responsive schizophrenic diblock copolymer.* Chemical Communications, 2002: p. 2122 - 2123.
12. Zhang, Z., et al., *Superlow Fouling Sulfobetaine and Carboxybetaine Polymers on Glass Slides.* Langmuir, 2006. **22**(24): p. 10072-10077.
13. Georgiev, G.S., Z.P. Mincheva, and V.T. Georgieva, *Temperature-sensitive polyzwitterionic gels.* Macromolecular Symposia, 2001. **164**(1): p. 301-312.
14. Lowe, A.B. and C.L. McCormick, *Synthesis and Solution Properties of Zwitterionic Polymers.* Chemical Reviews, 2002. **102**(11): p. 4177-4190.
15. Huglin, M.B. and M.A. Radwan, *Unperturbed dimensions of a zwitterionic polymethacrylate.* Polymer International, 1991. **26**(2): p. 97-104.
16. Kamenova, I., et al., *Swelling of the Zwitterionic Copolymer Networks and Dehydration of their Hydrogels.* Macromolecular Symposia, 2007. **254**(1): p. 122-127.
17. Friedman, H.L., *Kinetics of thermal degradation of char-forming plastics from thermogravimetry-application to a phenolic resin.* Journal of polymer Science, 1964. **6C**: p. 183.
18. Kasák, P., et al., *Zwitterionic hydrogels crosslinked with novel zwitterionic crosslinkers: Synthesis and characterization.* Polymer, 2011. **52**(14): p. 3011-3020.
19. Chang, Y., et al., *Tunable Bioadhesive Copolymer Hydrogels of Thermoresponsive Poly(N-isopropyl acrylamide) Containing Zwitterionic Polysulfobetaine.* Biomacromolecules, 2010. **11**(4): p. 1101-1110.
20. Schild, H.G., *Poly(N-isopropylacrylamide): experiment, theory and application.* Progress in Polymer Science, 1992. **17**(2): p. 163-249.

21. Singhal, R., R. Tomar, and A. Nagpal, *Effect of cross-linker and initiator concentration on the swelling behaviour and network parameters of superabsorbent hydrogels based on acrylamide and acrylic acid.* International Journal of Plastics Technology, 2009. **13**(1): p. 22-37.
22. Xie, J., et al., *Swelling properties of superabsorbent poly(acrylic acid-co-acrylamide) with different crosslinkers.* Journal of Applied Polymer Science, 2009. **112**(2): p. 602-608.
23. Baker, B.A., R.L. Murff, and V.T. Milam, *Tailoring the mechanical properties of polyacrylamide-based hydrogels.* Polymer, 2010. **51**(10): p. 2207-2214.
24. Zhu, X., et al., *The Synthesis and Characteristic Properties of Poly (AAc-co-AAm).* Advanced Materials Research, 2011. **213**: p. 534.
25. Klenina, O.V. and E.G. Fain, *Phase separation in the system polyacrylic acid-polyacrylamide-water.* Polymer Science U.S.S.R., 1981. **23**(6): p. 1439-1446.
26. Osada, Y., *Equilibrium study of polymer–polymer complexation of poly(methacrylic acid) and poly(acrylic acid) with complementary polymers through cooperative hydrogen bonding.* Journal of Polymer Science: Polymer Chemistry Edition, 1979. **17**(11): p. 3485-3498.
27. Painter, P.C., J. Graf, and M.M. Coleman, *A lattice model describing hydrogen bonding in polymer mixtures.* The Journal of Chemical Physics, 1990. **92**(10): p. 6166-6174.
28. Klenina, O.V., et al., *Phase separation in the hydrolyzed polyacrylamide-water-hydrochloric acid system.* Kolloidnyi Zhurnal, 1980. **42**(3): p. 558-561.
29. Tanaka, T., et al., *Phase Transitions in Ionic Gels.* Physical Review Letters, 1980. **45**(20): p. 1636.
30. Aoki, T., M. Kawashima, H. Katono, K. Sanui, N. Ogata, T. Okano, Y. Sakurai, *Temperature-Responsive Interpenetrating Polymer Networks Constructed with Poly(acrylic acid) and Poly(N,N-dimthylacrylamide).* Macromolecules, 1994. **27**: p. 947 - 952.
31. Day, J. and I. Robb, *Thermodynamic parameters of polyacrylamides in water.* Polymer, 1981. **22**: p. 1530.
32. Briscoe, B., P. Luckham, and S. Zhu, *On the effects of water solvency towards non–ionic polymers.* Proceedings of the Royal Society of London. Series A: Mathematical, Physical and Engineering Sciences, 1999. **455**(1982): p. 737-756.
33. Ilmain, F., T. Tanaka, and E. Kokufuta, *Volume transition in a gel driven by hydrogen bonding.* Nature, 1991. **349**(6308): p. 400-401.
34. Cecil, R., *Model System for Hydrophobic Interactions.* Nature, 1967. **214**(5086): p. 369-370.
35. Yang, M., et al., *Temperature-Responsive Properties of Poly(acrylic acid-co-acrylamide) Hydrophobic Association Hydrogels with High Mechanical Strength.* Macromolecules, 2010. **43**(24): p. 10645-10651.
36. Tanaka, T., *Collapse of Gels and the Critical Endpoint.* Physical Review Letters, 1978. **40**(12): p. 820.
37. Tanaka, T., *Phase transitions in gels and a single polymer.* Polymer, 1979. **20**(11): p. 1404-1412.

38. Katono, H., et al., *Thermo-responsive swelling and drug release switching of interpenetrating polymer networks composed of poly(acrylamide-co-butyl methacrylate) and poly (acrylic acid).* Journal of Controlled Release, 1991. **16**(1-2): p. 215-227.
39. Seuring, J. and S. Agarwal, *Non-Ionic Homo- and Copolymers with H-Donor and H-Acceptor Units with an UCST in Water.* Macromolecular Chemistry and Physics, 2010. **211**(19): p. 2109-2117.
40. Sasase, H., et al., *Regulation of temperature-response swelling behavior of interpenetrating polymer networks composed of hydrogen bonding polymers.* Die Makromolekulare Chemie, Rapid Communications, 1992. **13**(12): p. 577-581.
41. Katono, H., Kohei Sanui, Naoya Ogata, Teruo Okano and Yasuhisa Sakurai, *Drug Release OFF Behavior and Deswelling Kinetics of Thermo-Responsive IPNs Composed of Poly(acrylamide-co-butyl methacrylate) and Poly(acrylic acid).* Polymer Journal, 1991. **23**(10): p. 1179 - 1189.
42. Singhal, R. and I. Gupta, *A Study on the Effect of Butyl Methacrylate Content on Swelling and Controlled-Release Behavior of Poly (Acrylamide-co-Butyl-Methacrylate-co-Acrylic Acid) Environment-Responsive Hydrogels.* International Journal of Polymeric Materials, 2010. **59**(10): p. 757-776.
43. Shibanuma, T., et al., *Thermosensitive Phase-Separation Behavior of Poly(acrylic acid)-graft-poly(N,N-dimethylacrylamide) Aqueous Solution.* Macromolecules, 1999. **33**(2): p. 444-450.
44. McCormick, C.L., et al., *RAFT-synthesized diblock and triblock copolymers: thermally-induced supramolecular assembly in aqueous media.* Soft Matter, 2008. **8**: p. 1760.
45. Hochberg, A., T. Tanaka, and D. Nicoli, *Spinodal Line and Critical Point of an Acrylamide Gel.* Physical Review Letters, 1979. **43**(3): p. 217-219.
46. Duran, S., D. Solpan, and O. Güven, *Synthesis and characterization of acrylamide-acrylic acid hydrogels and adsorption of some textile dyes.* Nuclear Instruments and Methods in Physics Research Section B: Beam Interactions with Materials and Atoms, 1999. **151**(1-4): p. 196-199.
47. Katime, I., et al., *Theophylline release from poly(acrylic acid-co-acrylamide) hydrogels.* Polymer Testing, 1999. **18**(7): p. 559-566.
48. Zhou, X., et al., *Investigation of pH sensitivity of poly(acrylic acid-co-acrylamide) hydrogel.* Polymer International, 2003. **52**(7): p. 1153-1157.
49. Chu, L.-Y., et al., *Negatively Thermoresponsive Membranes with Functional Gates Driven by Zipper-Type Hydrogen-Bonding Interactions.* Angewandte Chemie International Edition, 2005. **44**(14): p. 2124-2127.
50. Haas, H.C., R.D. Moreau, and N.W. Schuler, *Synthetic thermally reversible gel systems. II.* Journal of Polymer Science, Polymer Physics Edition, 1967. **5**(5): p. 915-927.
51. Haas, H.C., C.K. Chiklis, and R.D. Moreau, *Synthetic thermally reversible gel systems. III.* Journal of Polymer Science Part A-1: Polymer Chemistry, 1970. **8**(5): p. 1131-1145.

52. Haas, H.C., R.L. MacDonald, and A.N. Schuler, *Synthetic thermally reversible gel systems. IV.* Journal of Polymer Science Part A-1: Polymer Chemistry, 1970. **8**(5): p. 1213-1226.
53. Haas, H.C., M.J. Manning, and M.H. Mach, *Synthetic thermally reversible gel systems. V.* Journal of Polymer Science Part A-1: Polymer Chemistry, 1970. **8**(7): p. 1725-1730.
54. Haas, H.C., R.L. MacDonald, and A.N. Schuler, *Synthetic thermally reversible gel systems. VI.* Journal of Polymer Science Part A-1: Polymer Chemistry, 1970. **8**(12): p. 3405-3415.
55. Haas, H.C. and N.W. Schuler, *Thermally reversible homopolymer gel systems.* Journal of Polymer Science Part B: Polymer Letters, 1964. **2**(12): p. 1095-1096.
56. Seuring, J., S. Agarwal, and K. Harms, *N-Acryloyl glycinamide.* Acta Crystallographica Section E, 2011. **67**(8): p. o2170.
57. Nagaoka, H., N. Ohnishi, and M. Eguchi, *Thermoresponsive polymer and production method thereof*. 2007, Chisso Corporation: United States.
58. Ohnishi, N., et al., *Polymer having an upper critical solution temperature*. 2007, Nathional Institute of Advanced Industrial Science and Technology, Chisso Corporation: United States.
59. Glatzel, S., et al., *Well-defined synthetic polymers with a protein-like gelation behaviour in water.* Chemical Communications, 2010. **46**(25): p. 4517-2519.
60. Seuring, J., et al., *Upper Critical Solution Temperature of Poly(N-acryloyl glycinamide) in Water: A Concealed Property.* Macromolecules, 2011.

3. Experimental Setup

3.1 Materials

The following chemicals were purchased from Sigma Aldrich (St. Louis, MO, USA) and used as received: sodium phosphate (both monobasic and dibasic), sodium chloride (NaCl), acrylamide monomer (A8887), acrylic acid monomer (147230), butyl methacrylate monomer (235865), N,N'-methylene bis-acrylamide crosslinker (146072), diphenyl(2,4,6-trimethylbenzoyl)phosphine oxide/2 hydroxy-2-methylpropiophenone blend UV initiator (405663), 17β-estradiol (E8875), recombinant human insulin from yeast (91077C). Pure deionized water (18 mΩ/cm) was filtered using a Barnstead Diamond NANOpure water purification unit. Whatman grade 5 filter paper was purchased from VWR International (Radnor, Pennsylvania, USA) and 5 mil GBC® HeatSeal™ lamination pockets were purchased from Grand and Toy Canada.

3.2 Preparation of Hydrogel Coated Paper Discs

Two sizes of membranes were used for this work, 18 mm and 30 mm diameter paper discs were cut from Whatman #5 filter paper. The discs were conditioned at 23°C and 50% relative humidity for 24 hours before coated with either a random copolymer hydrogel or an IPN hydrogel.

3.2.1 Random Copolymer Coatings

Various amounts of Am, AA, BMA and MBAm were mixed into 15 mL of pure water as per Table 1 and Table 2 in glass vials. AA and BMA, although purchased in liquid form were measured by mass at 20°C. The solutions were bubbled with nitrogen gas for 20 minutes. 38 μL of UV initiator was suspended and dispersed in the monomer solution by agitation in a nitrogen environment. Paper discs were immersed in the aqueous monomer mixtures for 30 minutes. The monomer soaked discs were then laminated to isolate them from ambient oxygen during polymerization by UV-irradiation (3.30 mW/cm^2 intensity) in a custom chamber for 60 minutes. The coated discs were washed in pure water, changed daily, at 40°C under constant agitation for 4 days then at 15°C under constant agitation for 3 days. After the discs were washed they were dried at 23°C and 50% relative humidity for 24 hours before their final mass was recorded.

Coating recipe A1-1 was adapted from a hydrogel formulation used by Zhou et al. [1]. A2, A3 and A4 hydrogel coatings were variations of A1-1 examining changes in crosslinker concentration, Am:AA monomer ratio and monomer concentration respectively. Explanation for choice of monomer and crosslinker quantities used by Zhou were poorly justified in their own work and solely used in this work as a basis point for

examining the effects of changing variables in hydrogel formulation. A1 and A2 coatings used a 3.33 mol/L monomer concentration basis, which the total concentration of monomer did not exceed. The monomer basis of A3 and A4 coatings were changed as required by the experimental design. Results from the hydraulic permeability tests for the random copolymer coatings in series A were considered before the formulation of the IPN coatings in series A and all series B coatings.

Table 1: Feed compositions for random copolymer coatings in series A.

Coating	Am (g)	AA (g)	MBAm (g)
A1-1	1.7755	1.8899	0.010
A2-1	1.7754	1.8001	0.020
A2-2	1.7760	1.8011	0.005
A3-1	1.7751	2.6997	0.010
A3-2	2.6631	1.8003	0.010
A4-1	1.0653	1.0793	0.010
A4-2	0.5336	0.5446	0.010

Table 2: Feed composition for random copolymer coatings in series B.

Coating	Am (g)	AA (g)	BMA (mol%)	MBAm (mol%)
B1-1	1.7572	1.7818	1.00	0.13
B1-2	1.7396	1.7638	2.00	0.13
B1-3	1.7221	1.7468	3.00	0.13
B1-5	1.6868	1.7109	5.00	0.13
B2-0	1.0660	1.0811	0.00	1.00
B2-1	1.0552	1.0746	1.00	1.00
B2-2	1.0452	1.0609	2.00	1.00
B2-3	1.0344	1.0483	3.00	1.00

Three different formulations varying the BMA content were prepared of each of the random copolymer and IPN types while maintaining the same overall molar content (See Table 1and Table 3). B1 coatings had a monomer basis of 3.33 M while B2 had a monomer basis of 2.00 M. All pre-gel coating formulations in series B contained a 1:1 Am and AA molar monomer ratio. A 5 mol% BMA membrane coating (B1-5) was formulated for use specifically with adsorption testing.

3.2.2 Interpenetrating Network Coatings

The interpenetrating gel coating networks were prepared in a sequential method adapted from Katono et al. [2]. The initial gel and secondary gel coating mixtures were prepared separately. Amounts of Am, AA, BMA and MBAm were mixed into 15 mL of pure water, as per Table 3, in glass vials. Crosslinker was added at 0.50 mol% to each initial and secondary gel feed solutions. The monomer mixtures were then bubbled with nitrogen gas for 20 minutes before 19 μL of UV initiator was suspended and dispersed in the monomer solution by agitation in a nitrogen environment. The polymerization and washing procedures were the same as for the random copolymer coatings. After the discs coated with the initial gel were weighed, they were immersed in corresponding solutions of various AA and MBAm concentrations (see Table 3) for 30 minutes. The secondary AA gel coating mixtures were prepared the same as the initial gel coating mixtures. Washing and weighing procedure were the same as for the initial gel coatings. All IPN coatings in series B had a 2.0 M total monomer basis. A 5 mol% BMA membrane coating (B3-5) was formulated for use specifically with adsorption testing.

Table 3: Feed compositions for IPN coatings in series A and B.

	Initial Gel		Secondary Gel
Coating	Am (g)	BMA (mol%)	AA (g)
A5-1	0.5333	---	0.5391
A5-2	1.0678	---	1.0868
A5-3	1.6002	---	1.6247
A5-4	2.1324	---	2.1646
B3-1	1.0559	1.00	1.0710
B3-2	1.0450	2.00	1.0601
B3-3	1.0346	3.00	1.0520
B3-5	1.0129	5.00	1.0303

3.2.3 Mass Gain

Mean dry mass gain is reported for all membranes and wet mass gain is reported but only for select B series membranes. Mass gain is calculated for each coated membrane type following equation 1.

$$\% \Delta \overline{m} = \frac{\overline{m}_{coated} - \overline{m}_{substrate}}{\overline{m}_{substrate}} \times 100\% \qquad \mathbf{1}$$

All dry membranes where conditioned at 23°C, 50% RH and all wet (swollen) membranes were immersed in water for 4 hours at 23°C. Excess water was blotted from the wet membranes with filter paper before mass was measured.

3.3 Hydraulic Permeability Testing

All membranes were compacted for 80 minutes at constant flux (2.358 x 10^{-5} $m^3 \cdot [m^2 \cdot s]^{-1}$) before any testing. Hydraulic permeability testing was performed with single 30mm Ø membranes in a jacketed stirred cell membrane filtration module with a reservoir volume of 10 mL. A constant permeate flux of 2.358 x 10^{-5} $m^3 \cdot [m^2 \cdot s]^{-1}$ was used for all membranes save when testing the uncoated filter paper (7.074 x 10^{-5} $m^3 \cdot [m^2 \cdot s]^{-1}$). Temperature was modulated between 7.5°C and 50°C at a rate of ±0.95 °C/min. The resulting back pressure from the temperature change was recorded (with a lower measurement limit of 1 kPa). Three thermal cycles, each including one heating stage and one cooling stage, were performed for each membrane with the resulting pressure recorded.

3.3.1 Permeability Calculation

Permeability of the membrane was calculated as a Darcy permeability using a constant flux rate and recorded TMP shown in equation 2.

$$\kappa = \frac{J_v \cdot \mu(T) \cdot \ell}{TMP} \qquad \mathbf{2}$$

The coated membranes were measured to have a thickness of 150 μm. The difference in thickness of dry and wet coated membranes was negligible. The dynamic viscosity was calculated using a formula from literature reported to have a maximum deviation of +/- 0.26% for water temperatures between -8°C and 150°C [3]. For the range of applied temperature, the viscosity of water was calculated to be between 0.001407 Pa·s and 0.000547 Pa·s.

The permeability values calculated in this work are a close approximation of permeability intended to provide some quantification to an otherwise qualitative study. A calculation of permeability incorporating dynamic changes in membrane thickness, pore tortuosity and surface functionality would provide a more accurate representation of the permeability response to temperature of the hydrogel coated membranes, but their measurement was decided to be impractical for the scope of this work. It is understood that these factors do affect the permeability of the membrane and that the 150 μm thickness value used would not always be accurate. These un-modeled parameters are therefore considered to be embedded in the Darcy permeability values calculated.

3.4 Adsorption (Binding) Test Procedure

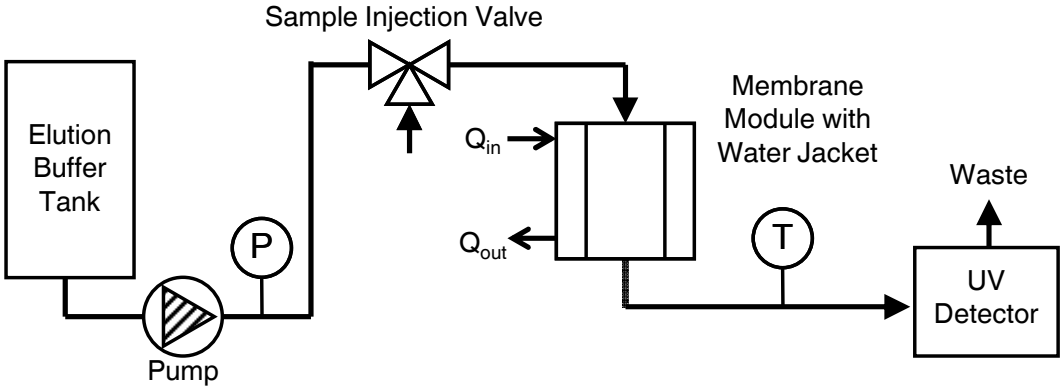

Figure 1: Equipment diagram for membrane adsorption

Adsorption tests were performed using a setup depicted in Figure 1. The pump maintained a constant PBS flow rate of 1 ml/min with pressure variation recorded through system back pressure. The sample injection valve was connected to a sample loop, injection volumes of 2 mL and 5 mL were used. The water jacket on the membrane module was controlled so that the resulting temperature of the effluent was in the range of 10°C to 45°C. The effluent from the module was fed into a UV absorbance detector set to a UV wavelength of 280 nm. The membrane module used for adsorption testing was different than the one used for hydraulic permeability testing. Hydraulic permeability testing used a stirred cell module while the binding tests used a dead-end stack module. Stacks of single 18 mm Ø membranes were considered for the binding tests. All membranes were soaked in pure water for 24 hours prior to use.

UV absorbance signals were allowed to settle over 160-240 minutes of flow with heating and cooling switching every 40 minutes until a steady detection baseline was established. Sample injections were performed in cold state (10.02 ± 0.01 °C), with heating, and hot state (43.35 ± 0.01 °C), with cooling, pairs with a total of four injections per membrane. Binding tests using the 2 mL sample injection loop allowed for 6 minutes of isothermal flow before temperature change while binding tests using the 5 mL sample injection loop allowed for 11 minutes of isothermal flow before temperature change. A heating and cooling cycle was applied over 80 minutes between all injection pairs to flush the membrane. The heating and cooling rates of all temperature cycles were 0.799 ± 0.014 °C/min and -0.857 ± 0.011 °C/min respectively.

3.4.1 Background Electrolyte Buffer Preparation

A phosphate buffer solution (PBS) consisting of both monobasic (8 mM) and dibasic (12 mM) sodium phosphate salts as well as NaCl (750 mM) was prepared in water as electrolyte buffer. The salt solution was filtered by cellulose acetate membrane, degassed

by vacuum and normalized to pH 7.2. All PBS prepared in this study contained the same concentrations of sodium phosphates with the amount of NaCl denoted when mentioned.

3.4.2 Injection Sample Preparation

A 1.0 µg/mL solution of E2 was prepared at 20°C in 250 mM NaCl PBS at pH 7.2. The aqueous solubility of E2 has been reported over a range of values however solubility strongly depends on solution conditions [4-7]. The solution criteria from Shareef et al. were used to determine the solution conditions of this prepared sample. The human insulin sample was prepared in similar PBS at pH 7.0 at a concentration of 10 µg/mL [8].

3.4.3 Hormone binding

The extend of binding of both E2 and human insulin were determined by injecting a pulse of aqueous sample at a steady temperature. The amount of hormone injected was in excess of the assumed saturation binding capacity of the membranes giving a flow-through fraction as well as an elution fraction. The fractions were detected in real time by UV absorbance. The absorbance peaks were subsequently evaluated by trapezoid rule with their values being related back to reference integrations of known injection concentrations using equation 3. The approximate quantity of compound in the flow-through fraction could then be inferred. The adsorption capacities of the membranes are reported as retention mass normalized to the surface area of the membrane.

$$\text{Retention} = \frac{\text{Flow - Through Integration}}{\text{Reference Flow - Through Integration}} \times \text{Known Injection Amount} \qquad 3$$

3.5 Environmental Scanning Electron Microscope (ESEM) Imaging

Environmental scanning electron microscope (ESEM) images were taken of various coated membranes as well as the uncoated Whatman filter paper. Samples were imaged using an electrically cooled cold-phase sample plate at 5°C. Pressure in the imaging chamber was modulated between 5.5 and 7.4 tor allowing both dry and wet conditions to be observed. Not all coated membranes were imaged. Membranes were chosen in the attempt to display visual differences in hydrogel dispersion, coating microstructure and coating composition.

3.6 Wet Strength Testing

The wet strength of the coated paper was examined by strain rate using an Instron 4411. Coated paper samples were cut into 25 mm long by 15 mm wide strips with an effective gauge length of 15 mm. Strain was recorded at an applied elongation rate of 2 mm/min

over 2 minutes. Four samples were tested for each coating formula; these samples were separate from the membranes used in the hydraulic permeability testing.

3.7 Chapter References

1. Zhou, X., et al., *Investigation of pH sensitivity of poly(acrylic acid-co-acrylamide) hydrogel.* Polymer International, 2003. **52**(7): p. 1153-1157.
2. Katono, H., et al., *Thermo-responsive swelling and drug release switching of interpenetrating polymer networks composed of poly(acrylamide-co-butyl methacrylate) and poly (acrylic acid).* Journal of Controlled Release, 1991. **16**(1-2): p. 215-227.
3. Kestin, J., M. Sokolov, and W.A. Wakeham, *Viscosity of Liquid Water in the Range -8°C to 150°C.* Journal of Physical Chemistry Reference Data, 1978. **7**(3): p. 941.
4. Hurwitz, A.R. and S.T. Liu, *Determination of aqueous solubility and pKa values of estrogens.* Journal of Pharmaceutical Sciences, 1977. **66**(5): p. 624-627.
5. Kabasakalian, P., E. Britt, and M.D. Yudis, *Solubility or some steroids in water.* Journal of Pharmaceutical Sciences, 1966. **55**(6): p. 642-642.
6. Shareef, A., et al., *Aqueous Solubilities of Estrone, 17β-Estradiol, 17α-Ethynylestradiol, and Bisphenol A.* Journal of Chemical & Engineering Data, 2006. **51**(3): p. 879-881.
7. Yu, Z., et al., *Sorption of steroid estrogens to soils and sediments.* Environmental Toxicology and Chemistry, 2004. **23**(3): p. 531-539.
8. *Product Information: Insulin, Recombinant Human*, in *Sigma Aldrich*. 2006, SAFC Biosciences: Lenexa.

4. Results & Discussion

4.1 Synthesis and characterization of paper membranes coated with thermo-responsive hydrogels

4.1.1 Series A Membranes

Figure 1 shows the results of the coating polymerization for all the formulations in series A in terms of percentage mass gain. Mass gain results are discussed in sections below.

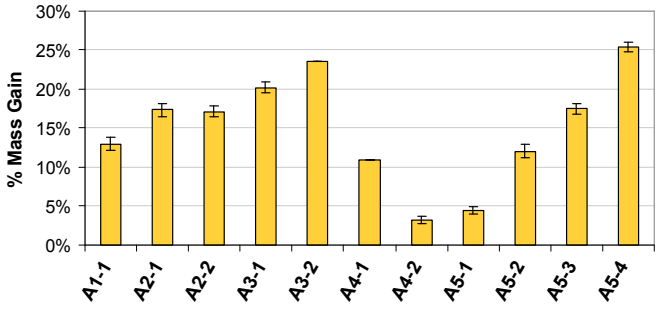

Figure 1: A-Series membrane coating polymerization results. Dry mass gain shown only.

Whatman filter paper has a reported Herzberg filtration speed with a Darcy permeability equivalent of 1.44×10^{-14} m^2 which could only be examined at water fluxes greater than 5.89×10^{-5} $m^3 \cdot [m^2 \cdot s]^{-1}$ with the experimental setup described above. Lower water flux did not give data within the sensitivity range of the apparatus. From Figure 2 it can be seen that the uncoated filter paper initially achieved the manufacturer reported permeability value but over time and thermal cycling, the membrane permeability decreased to 1% of its initial value. This is indicative of membrane compaction. There was also apparent response to temperature by the uncoated membrane but from the decreasing trend and convergence between hot and cold state permeability values, it is expected that significant temperature response would cease to be apparent after sufficient filter compaction.

The A1-1 coated membrane displayed an inverse permeability response to temperature depicted in Figure 3. After initial compaction instability in the first cycle, the permeability of the membrane stabilized between 0.74×10^{-17} m^2 and 1.27×10^{-17} m^2 as the temperature was cycled between 7.8°C and 44.8°C. The start-up instability was consistent through all hydraulic permeability tests and not represented in the steady state permeability data shown in Table 1. Capability of the hydrogel coatings was considered primarily by the overall magnitude and range of Darcy permeability values. High and low

permeability is reported as the mean of values at corresponding high and low temperatures.

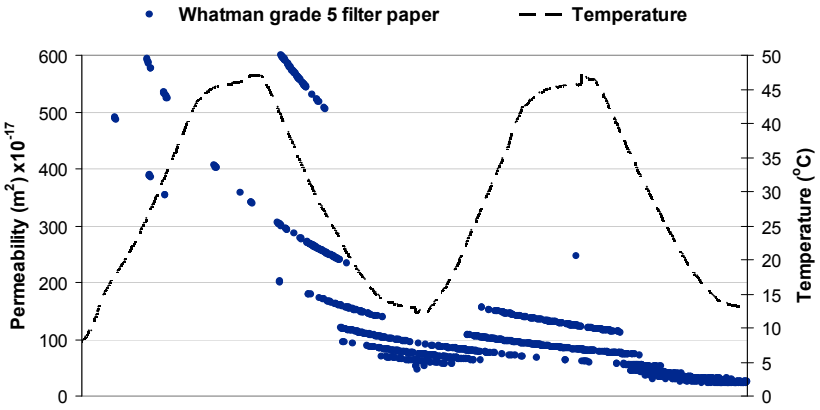

Figure 2: Permeability profile of uncoated Whatman grade 5 filter paper through two temperature cycles at an elevated water flux.

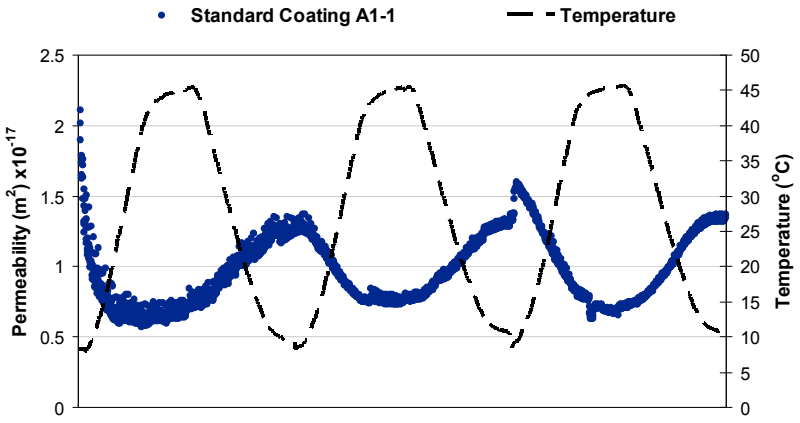

Figure 3: Permeability of A1-1 coating formulation, adapted from Zhou et al., through three temperature cycles.

The first variation in the pre-gel solution formulation that was examined was the effect of crosslinking agent. It was hypothesized that higher inclusion of MBAm would promote greater reversibility of the PVT and would manifest itself in the permeability testing as consistent minimum and maximum permeability values. This hypothesis is based on the assumption that the crosslinks will be well distributed and will impart consistent structure to the gel network, reducing the length of polymer segments and degree of rearrangement of the polymer chains that could occur in swollen states of the hydrogel [1, 2]. The amount of MBAm in A2-1 is doubled to 20 mg while the MBAm content in A2-2 is halved to 5 mg. The crosslinker content did not affect the mass gain of the composite membranes significantly (see Figure 1) however the magnitude of permeability change

and the absolute range differed drastically. The higher MBAm inclusion in the pre-gel formulation promoted better defined permeability changes but a higher TMP across the membrane.

Table 1: Summary of permeability for random copolymer coated membrane in Series A.

	Temperature (°C)		Permeability (m^2) x10^{-17}		
Coating	$\overline{T}$ (high)	$\overline{T}$ (low)	$\overline{\kappa}$ (high)	$\overline{\kappa}$ (Low)	Range
A1-1	44.8	7.8	1.27	0.74	0.53
A2-1	44.1	9.3	0.84	0.45	0.39
A2-2	44.9	7.8	2.52	1.32	1.21
A3-1	45.0	9.6	0.90	0.40	0.49
A3-2	41.7	7.9	0.99	0.51	0.49
A4-1	44.6	9.6	9.55	7.09	2.45
A4-2	44.8	9.7	30.88	15.79	15.09

Formulations A3-1 and A3-2 modify the ratio of co-monomers in the pre-gel mixtures. A3-1 uses a 2:3 ratio of Am to AA and A3-2 uses a 3:2 ratio of Am to AA. This differs from the standard 1:1 ratio in A1-1. The equimolar 1:1 ratio represents the ideal system where one amide unit interacts with one carboxyl unit. This concept has been shown in aqueous polymer solutions [3] and is used regularly by other workers as the standard for hydrogel synthesis [4, 5]. Am and AA interact with each other based on hydrogen bonding between the amide group of Am and the carboxyl group on AA shown in Figure 4. Monomer sequence inconsistencies may arise in polymer segments and amide groups are also capable of interacting with themselves which can leave some AA units unpaired. Amide interactions with other amides are not as thermally responsive as amide-carboxyl interactions and can reduce the magnitude of the volume-phase transition. A higher AA concentration in the pre-gel formulation would ensure excess carboxyl units, decreasing the opportunity for the formation of amide-amide complexes. Conversely, a higher Am concentration in the pre-gel formulation could possibly reduce the chance of unpaired carboxyl units even with increased chance of amide-amide complex formation. This has been examined by others [4, 6].

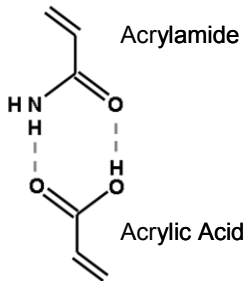

Figure 4: Hydrogen bonding between the amide and carboxyl groups of acrylamide and acrylic acid.

Results from the hydraulic permeability testing for both A3-1 and A3-2 coated membrane formulations yielded inconclusive temperature response profiles although both coating formulations yielded membranes with similar mass gain. This was reflected in the reduced permeability of both membrane types compared to A1-1. The A3-1 membrane did not stabilize through two temperature cycles and was inconsistent through an additional three cycles. The overall permeability continued to decrease with successive heating and cooling stages. The A3-1 and A3-2 formulations were the only pre-gel solutions to unintentionally exceed the 1.665 M basis that was maintained for all other A-series formulations. While one monomer concentration was kept constant, the other was raised to 2.5 M to meet the intended 2:3 ratio. This is what was assumed to be responsible for the higher mass gains of the A3 coatings. Small deviations from the 1:1 Am-AA ratio or changes in crosslinker content less than 1.00 mol% did not appear to greatly affect the functionality of the coated membranes. These factors should be used to fine-tune the performance of the hydrogel coatings for specific end-use capability.

Monomer concentration and subsequently, loading of the hydrogel coating onto the filter paper substrate, was the focus of the A4 formulations. The monomer concentration basis was reduced in A4-1 to 1.0 M and reduced again to 0.5 M for A4-2. As was expected, the membrane mass gains were lessened by the diluted pre-gel mixtures as shown in Figure 1. Overall permeability increased inversely to the loading of the substrate and the responsiveness of the hydrogel coating became less apparent at higher loadings but the response profile gained better resolution. Mass gain was the dominating factor in determining the performance of the coated membranes. This result is actually very intuitive as the more hydrogel that is polymerized throughout the cellulose network of the filter paper, the less void space there is in the filter paper and the lower the overall permeability. Also clarity of the permeability response profile can be explained this way as well. With a lower hydrogel loading in the paper cellulose structure there are larger pore spaces to be occupied and then vacated as the hydrogel swells and collapses. These large pore spaces would have a broader size distribution and would be less consistently filled than a membrane with a higher degree of gel loading and smaller pore spaces. A

distribution of smaller pores can be more consistently filled by a greater amount of hydrogel than can a distribution of larger pores by a lesser amount of hydrogel.

The A5 formulations represent the IPN coatings. The IPN formulations were investigated by changing monomer concentration while keeping crosslinker content and monomer ratio constant. A5-1 used a 0.5 M monomer basis in the pre-gel mixture and was increased by increments of 0.5 M for each coating until reaching a maximum of a 2.0 M basis for A5-4. As was expected, the loading of the hydrogel coating increased with higher monomer concentration as before, decreasing overall permeability at each increment. A5-4 did not consistently provide TMP below the upper measurement threshold of the apparatus. Table 2 shows the permeability displayed by A5-1, A5-2 and A5-3. Similar to the random copolymer A4 coatings, the membrane with the lowest loading not only shows the greatest permeability, but also the responsiveness became less defined, providing greater signal variability during flow. Both A5-2 and A5-3 displayed good reversibility.

Referring again to Table 2, it can be seen that the magnitude of permeability decreases significantly at each incremental increase of monomer concentration in the pre-gel mixture. Of note is that the IPN coated membranes did not experience an abrupt PVT when heated. The behaviour of the IPN membranes mirrored the swelling profiles exhibited by the random copolymer membranes. Coating microstructure was not seen to provoke a significant difference in permeability response for the membranes although some discrepancies in the results suggest this should be investigated further as IPN coated membranes didn't strictly adhere to the overarching trend of greater membrane mass gain translating to lower overall permeability.

Table 2: Summary of permeability for IPN coated membranes in Series A.

Coating	Temperature (°C)		Permeability (m^2) x10^{-17}		
	$\overline{T}$ (high)	$\overline{T}$ (low)	$\overline{\kappa}$ (high)	$\overline{\kappa}$ (Low)	Range
A5-1	44.2	9.1	36.28	17.04	19.24
A5-2	43.5	8.8	12.07	7.81	4.26
A5-3	44.3	9.3	0.87	0.46	0.41

4.1.2 Series B Membranes

Series B featured coated membranes modified with BMA that were based on three select formulations from Series A. Formulations were selected for their overall permeability and clarity of their response to temperature. Coated membranes that had a higher overall permeability typically did not follow a well defined permeability change profile, often

having large distortions due to possible non-uniform loading of the hydrogel on the membrane. Formulations that used higher pre-gel monomer concentrations produced better defined permeability profiles but at too high of a concentration, permeability was decreased enough that the pump system became strained. Formulations that were based on 2.0 M and 3.33 M total monomer concentrations were selected for BMA modification in Series B, specifically A1-1 and A5-2. An additional formulation was developed using the findings from Series A, a random copolymer coating formula with a 2.0 M total monomer concentration basis labelled B2-0. The MBAm content was increased to 1.0 mol% for this recipe, reflecting both the asserted benefits of higher crosslinker concentration in literature and the findings of this study [1, 2]. B1 formulations are extensions of A1-1 and B3 formulations of A5-2. The second number in the formulation label refers to the molar percent of BMA incorporated into the pre-gel mixture while keeping the total moles of monomer consistent. B1-1 incorporates 1 mol% BMA into the A1-1 formulation while B1-2 incorporates 2 mol%, where the total number of molar composition of monomer doesn't exceed 3.33 M. Figure 5 shows the dry and swollen mass gain of each formulation in Series B. A1-1 has bee relabelled "B1-0" and A5-2 has been relabelled "B3-0". Category B1 formulations generally showed increasing dry hydrogel loading and greater wet mass with higher BMA content while B2 and B3 displayed a decrease of dry mass loading and wet mass with BMA content. The difference between dry and wet mass loading is indicative of the extent of swelling of the coating.

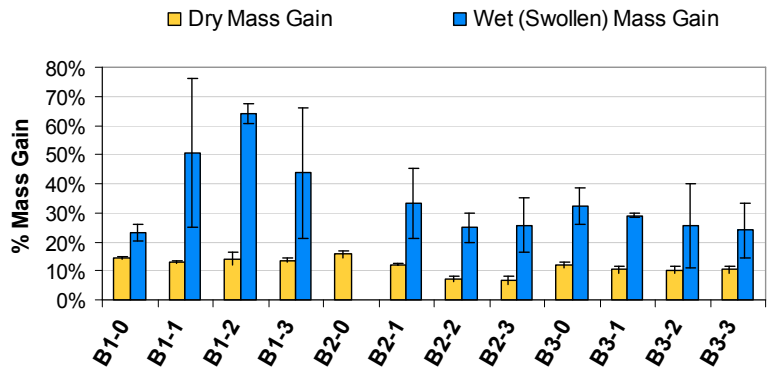

Figure 5: B-series coated membrane polymerization results. Dry and wet mass gains.

BMA inclusion as stated earlier should increase the volume-phase transition temperature of the hydrogel. More hydrophobic inclusion leads to further increase of the transition temperature. This gives us the ability to either raise the temperature range that we wish the membrane to perform under or decrease the PVT response of the membranes at the same temperatures. The permeability results for B1 and B2 coated membrane categories have one trend anomaly each while the IPN coated membranes in B3 displayed the

expected trend. From Table 3, the overall magnitude of permeability response increases with the first addition of BMA at 1 mol% to A1-1, which is the anomaly, but then, settles into the expected trend of decreasing magnitude. Referring to the mass loadings of B1 coatings in Figure 5, the wet mass loading reflects the range of permeability change and is similar to the changes in magnitude.

Table 3: Summary of permeability for coated membranes in Series B.

	Temperature (°C)		Permeability (m^2) x10^{-17}		
Coating	$\overline{T}$ (high)	$\overline{T}$ (low)	$\overline{\kappa}$ (high)	$\overline{\kappa}$ (Low)	Range
B1-0	44.8	9.7	1.27	0.74	0.53
B1-1	40.6	8.8	3.93	2.20	1.73
B1-2	48.7	8.8	3.68	1.82	1.86
B1-3	46.6	8.6	1.37	0.88	0.48
B2-0	40.8	7.8	3.59	2.53	1.06
B2-1	48.5	7.9	2.62	1.57	1.05
B2-2	49.0	8.1	3.58	2.05	1.53
B2-3	49.2	9.7	4.23	3.54	0.69
B3-0	43.5	8.8	12.07	7.81	4.26
B3-1	48.0	8.3	9.03	5.98	3.05
B3-2	48.7	7.9	7.89	5.65	2.24
B3-3	49.5	8.7	5.20	3.01	2.20

For the B2 formulations, it can be observed that both the magnitude and the range of response decreases with 1 mol% BMA inclusion of the 1.0 M basis random copolymer coating but then begins to increase at 2 mol% and 3 mol% finally giving a permeability response that is greater in magnitude than the base B2-0 coating. The trend anomaly in the B2 coatings is the inflection point for BMA inclusion where permeability response changed from a decreasing trend to an increasing one. Reference to the mass loadings of the B2 coatings gives some explanation as the average membrane mass gain decreases with higher BMA inclusion in the pre-gel formulas. From earlier results we have shown that lower membrane mass gains will supersede the chemical responses of the hydrogel coating and have a stronger influence on the magnitude and range of permeability and this case appears to be no different.

From first look, the permeability magnitudes for the IPN coatings in the B3 formulations follow the mass loading trend observed in the A-series coatings. As well, a consistent increase of mass loading was seen with increasing BMA inclusion. Both points seem to

reaffirm that mass loading of the hydrogel coating onto the substrate superseded the effect of volume-phase transition chemistry on permeability response of the composite membrane. The resolution of the permeability response didn't maintain a trend with increasing or decreasing membrane mass gain nor did the IPN microstructure of the hydrogel coating appear to affect the kinetics of response, which is consistent from the IPN coatings in series A.

The range of permeability change for both B1 and B2 coatings decreases at 3 mol% BMA content. This is likely observation of the predicted effect of BMA on the interactions between Am and AA units. Resolution of the permeability response was improved through incorporating BMA in the coating formula however differences between the degrees of inclusion weren't consistent enough to determine any trending result. Although the magnitude of permeability change between hot and cold phases did generally increase through BMA inclusion. One large difference that was observed between the A-series and B-series coatings is that the coatings with hydrophobic monomer units maintain better clarity of permeability response at lower mass loadings than those without.

4.2 Estradiol adsorption potential of thermo-responsive membranes in low salt solution

4.2.1 Membrane Behaviour and Effect of Module Selection

From the preparatory thermal cycles applied to the membranes before adsorption sample injections, described in Chapter 3, hydraulic permeability behaviour was again observed. All tested membranes displayed an abrupt hydraulic permeability shift upon temperature change, occasionally becoming smoother after extensive thermal cycling. The permeability change observed was inversely related to temperature change similar to the stirred cell tests, decreasing with heating and increasing with cooling. The same membrane performing in the two modules produced drastically different results. The scale of permeability improved greatly in the dead-end stack module and the permeability shift on temperature change occurred abruptly and to a greater extent than was seen in the stirred cell module. Figure 6 exhibits the response of membranes B1-1 and B3-2 as examples in each module type and while not shown, B1-2 and B3-1 displayed similar behaviours.

It is known that differentiations of design within the same membrane module type induce slightly different behaviour from the applied membranes, enabling module design optimization [7]. However there are few reports directly comparing differentiating behaviour of the same membrane in different modules. Through the conduct of this project, two module types were used, a stirred cell module and a dead-end stack module. The primary differences between the two modules are membrane chamber volume and

feed turbulence. The depth of the permeate reservoir of a stirred cell module is much larger than the depth of the membrane bed, effectively allowing the membrane depth to fluctuate freely. It also maintains a high permeate turbulence from the stirring baffles. The dead-end module maintains a fixed membrane bed depth and low permeate turbulence. In relation to this project, the module differences manifested as significantly different permeation profiles with respect to temperature. Results from stirred cell module appeared to be affected more by the changing viscosity of water while the dead-end module did not. The stirred cell module generally reported lower permeability and more gradual permeability change for the same membranes under the same heating and cooling rates than with the dead-end modules.

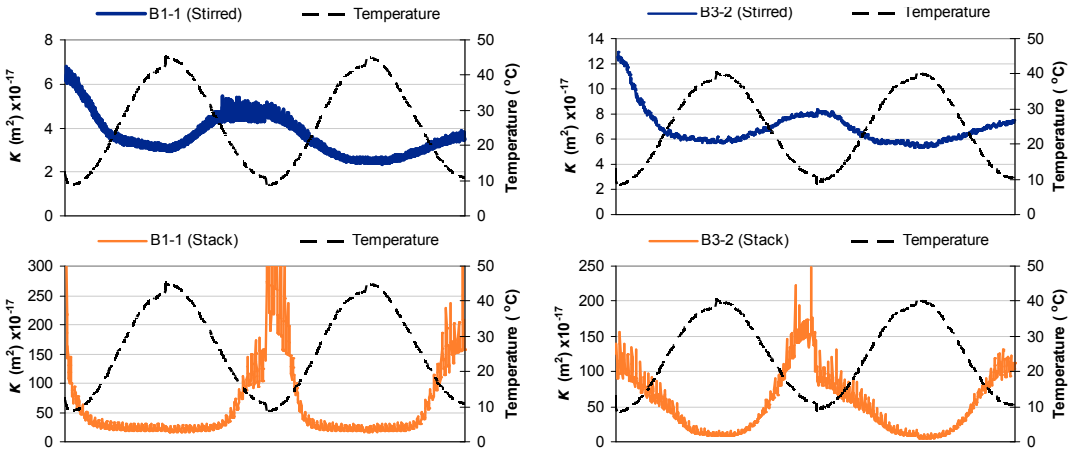

Figure 6: Comparative plots of permeability response to temperature for membranes B1-1 and B3-2 for both a stirred cell module and a dead-end stack module.

4.2.2 Estradiol Adsorption

Table 4 shows the mean mass gain of hydrogel on the membranes used for E2 adsorption testing. The reported mean mass gain is the result of three to seven membrane coating syntheses. The IPN membranes had an overall lesser loading of hydrogel, most likely due to the lesser molar amount of monomer used in their pre-gel formulas. Mass gain increased in both cases with increasing BMA content which was expected as BMA has a larger molecular weight. Recall coated membranes B1-5 and B3-5 were specific to adsorption testing.

Table 4: Mass loading of hydrogel on membranes for adsorption testing.

Coating	Random Copolymer			IPN		
	B1-1	B1-2	B1-5	B3-1	B3-2	B3-5
$\%\Delta\overline{m}$	13.06 ± 0.37	14.15 ± 2.20	18.33 ± 0.71	10.43 ± 1.04	10.25 ± 1.10	12.55 ± 0.65

Retention of E2 was determined as the difference between the injected and flow-through quantities and was observed for all coated membranes at cold temperatures. The strongest performing membranes had an IPN coating, the best being B3-2 with E2 retention consistently being greater than 0.25 µg/cm^2. Figure 7 shows the E2 retention observed from all tested membranes. Random copolymer coatings and IPN coatings appeared to have distinct trends. Random copolymer coated membranes generally displayed a decreased retention of the second injection while IPN coated membranes displayed an increase in retention of the second injection. While a decreasing trend is indicative of mainly irreversible adsorption, small data populations and the increasing trend shown with the IPN coated membranes indicate the full adsorptive capability of the membranes was not observed in these tests. The median retention values of 0.176 µg/cm^2 and 0.174 µg/cm^2 for the first and second E2 injections respectively do not show a significant decline of adsorption between injections and support the assertion that the coated membranes would be capable of several more injections resulting in similar retention.

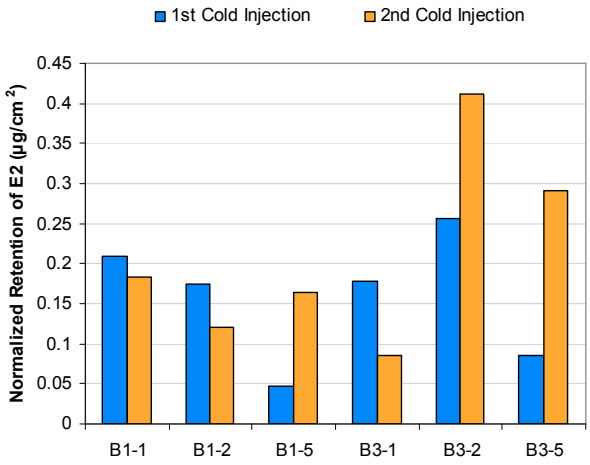

Figure 7: E2 retained by each membrane at cold temperatures, normalized to membrane area.

The majority of hot state E2 injections displayed a greater E2 content in the flow-through fraction than was injected, signifying either polymerization residue or previously bound E2 was desorbing from the membranes. This is reflected in Figure 8 by a negative E2 retention value. However, it is unlikely that the increased signal is due to residual polymerization compounds if they were not apparent in previous injection or flushing cycles. All flushing cycles immediately preceding injections were consistent with preparatory detection baselines, all lacking clear elution peaks. The increased flow-through fractions obtained for the hot state injections of most membranes suggests a delayed elution of bound E2 residual from the cold state injection prior. Only one

membrane, B3-5, displayed consistent reductions in E2 flow-through content at high temperature. This is likely from the increased potential for hydrophobic interactions enabled by a higher BMA content. Membrane B1-5 also showed a tendency for E2 retention at high temperature. Only one set of injection data is available for B3-1 due to equipment malfunction and no hot state injection information is available for B3-2 because of constantly poor absorbance detection.

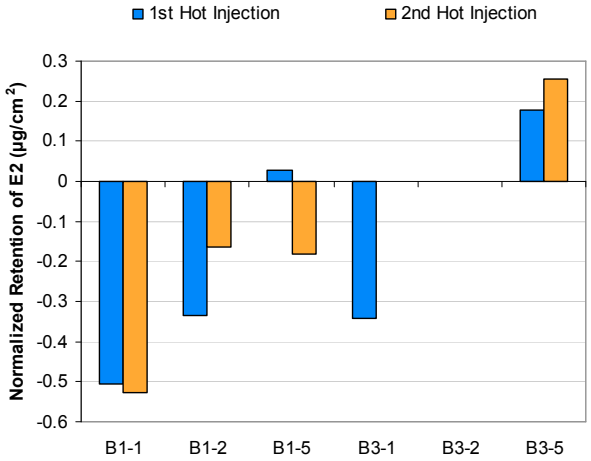

Figure 8: E2 retained by each membrane at hot temperatures, normalized to membrane area.

As puslatile sample injections were not repeated on new membranes of the same coating type, it was necessary to determine the statistical significance of the collected data for cold temperature and hot temperature binding tests. The null hypothesis that was used was 'E2 did not interact with the membrane in any way'. This was quantified by setting the expected sample flow-through fraction integration value equal to the mean of flow-through fraction value attained from control runs under non-binding conditions. In other words, the null hypothesis effective binding capacity was 0.0 µg/cm^2. The cold state and hot state data were compared individually against the non-binding condition data as unpaired data sets with unequal sample sizes and unequal variance in a two-tailed Student's t distribution test. The cold temperature adsorption data was determined to be statistically significant to the 99% confidence level denoting that perturbations in the UV absorbance signal are very likely indicative of a decrease in the flow-through fraction E2 concentration by the coated membranes. Confidence level decreased to 98% when the first and second cold temperature injections were compared separately suggesting cold temperature adsorption is still very likely. Perturbations in the hot temperature UV absorbance profiles for the flow-through fractions from the control values were determined to be much less statistically significant, only achieving an 85% confidence

level. This data was considered to have upheld the null hypothesis concurrent with the expectation that the swollen hydrogel coating would not interact with E2. Discussion of material being rejected from the membrane in excess of the injected sample is therefore purely speculative.

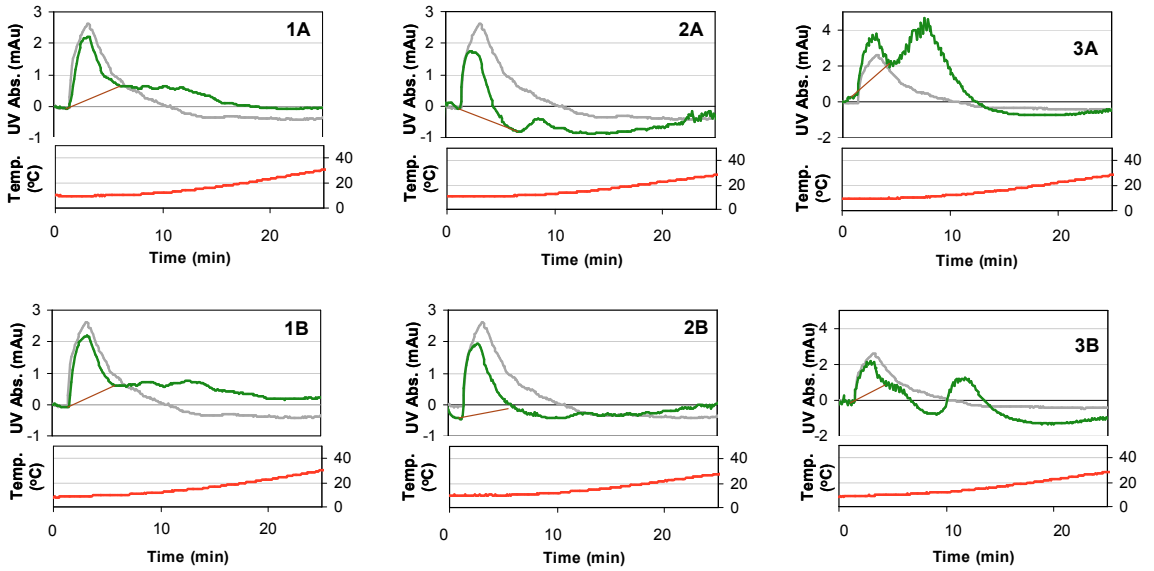

Figure 9: E2 flow-through UV absorbance signals. Shown are both the first and second cold state flow-through for coated membranes B1-1 (1A/B), B3-1 (2A/B) and B3-2 (3A/B). Membrane B1-1 shows significant peak widening while B3-1 and B3-2 both display an elution fraction. The integration baselines for the flow-through fractions are shown and E2 injection occurs at time = 0. A control UV absorbance signal for uncoated paper is provided in light grey for comparison in each graph.

Three membranes, B1-1, B3-1 and B3-2 produced an elution fraction or significant flow-through peak widening after the cold injections. Consistent elution fractions weren't observed after hot injections of any membrane. The flow-through peak widening was observed with membrane B1-1 to persist until 20 minutes after injection while elution peaks were seen from membranes B3-1 and B3-2 each at ~10 minutes after injection. UV absorbance profiles are shown in Figure 9. For membrane B1-1, the flow-through signal persists until the temperature reaches ~23°C when E2 has been fully flushed. For membranes B3-1 and B3-2, the second peak begins at membrane temperatures between 9.7°C and 12.8°C, returning to baseline absorbance levels between 14°C – 15.6°C for B3-1 and between 18.7°C – 19.9°C for B3-2. These temperatures all coincide with the reported Am-AA dissociation temperatures from literature stated above, although in the low-medium range, confirming that either adequate hydration is disrupting hydrophobic

interaction, or dissociation of hydrogen bonds is occurring without significant hindrance from BMA.

Integrating the elution fraction absorbance peaks for B3-2 reports misleading results as the sum of the flow-through fraction and the elution fraction is greater than the reference quantity of E2. The absorbance peak widening observed with B1-1 indicated that there were interactions occurring between the membrane and E2 however complete adsorption did not happen. B3-1 produced the best quantifiable elution fractions. The two cold temperature elution peaks from B3-1 correspond to 0.182 μg and 0.065 μg (or 40.3% and 29.8%) of the bound material respectively.

Binding runs performed with 5 mL E2 injection volume did not give additional information on binding capacity. The results of the binding runs performed with 2 mL E2 sample solution injection volumes suggest that the E2 concentration in the sample solution was in excess of the effective binding capacity of the coated membranes, which was intended. Since the E2 content of 2 mL of sample exceeded available binding sites, the E2 content of 5 mL of sample solution more than exceeded available binding sites resulting in negligible reductions of E2 in flow-through fractions. E2 reduction was only readily observed with coated membrane B3-2 which was 0.199 $\mu g/cm^2$ and 0.259 $\mu g/cm^2$ for two cold state injections. These values are consistent with the binding results from 2 mL sample injections where there is an increase of bound material upon successive injections of E2. The flow-through fractions of the hot state 5 mL E2 injections displayed similar results as with the 2 mL injections where the flow-through fractions recorded a greater absorbance signal than the control values.

The membranes with the lowest mass loading of hydrogel, B1-1, B1-2 and B3-2, displayed the most consistent adsorption of E2 as shown by relative reductions in the flow-through fractions. Other membranes, while sometimes exhibiting stronger adsorptive tendencies, were not consistent in their performance through several injections. The membranes with higher mass loadings typically did not perform as well. This is probably due to the hindering effect of increased diffusion transport. Researchers have often observed that diffusion is a slower mass transfer process than convection [8, 9]. More hydrogel loading of the membrane means diffusion gains a larger role for access of E2 to the binding sites. This translates into less adsorption given the same amount of time as a membrane with greater convective effects. Diffusion would be particularly hindering with these membranes at cold temperatures, when the hydrogel coating forms tight hydrogen-bonded complexes and becomes denser.

While both random copolymer and IPN coating types displayed the ability to reduce E2 content of the flow-through fractions, only the IPN coatings showed clear elution fractions. In the copolymer coating, functional Am, AA and BMA units would be

randomly distributed causing an equally random distribution of adsorption sites with some being easier to access than others. With flux and time being constant variables for each membrane, distinct elution fractions were not observed but it is possible that some or all random copolymer coated membranes could produce elution fractions given enough time. As mentioned earlier, the greater than unity flow-through fractions from the hot injections may contain this elution fraction from the cold adsorption. An IPN coating would produce more uniform polymer chains which provides a more equally distributed amount of adsorption sites. This contributes both in the adsorption and elution of E2 as the hydrogel dissociates faster and more evenly, discharging a larger amount of bound material in a shorter time.

4.2.3 Insulin Adsorption

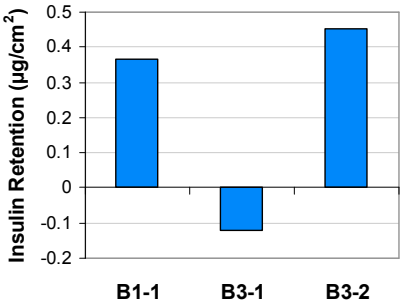

Figure 10: Insulin retained by each membrane at cold temperatures, normalized to membrane area.

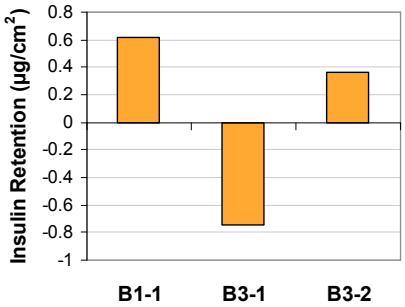

Figure 11: Insulin retained by each membrane at hot temperatures, normalized to membrane area.

After the binding results with E2, tests with human insulin considered only 2 mL injections with coated membranes B1-1, B3-1 and B3-2 as those membranes displayed the strongest interactions with E2. Cold insulin retention results per area of membrane are shown in Figure 10 and hot insulin retention results in Figure 11.

Membranes B1-1 and B3-2 displayed clear insulin retentions of 0.366 µg/cm^2 and 0.451 µg/cm^2 respectively at cold temperatures. Retention of insulin was also observed for the hot injection flow-through fractions of B1-1 and B3-2 which are dissimilar to the findings for their hot E2 injections. The insulin retention at hot temperatures were 0.618 µg/cm^2 for B1-1 and 0.364 µg/cm^2 for B3-2. It is unknown why flow-through fraction values for B3-1 were consistently well above the control values, giving negative retentions. Figure 12 shows possible elution fractions for B1-1 at cold temperature and both hot and cold temperatures for B3-2. The high retention of insulin for both cold and hot injection flow-through fractions and the absence of clear elution fractions suggest irreversible adsorption of the insulin to the membranes. However it is more likely that reduced pore sizes at the warmer temperatures and from the coating process in general had a size exclusion effect

as insulin is a much larger molecule than E2. This is more strongly indicated than irreversible adsorption by the increased retention of insulin at hot temperatures since the hydrogel coatings are known to reduce pore size at higher temperature. Although quantification of the insulin injection data was possible, it only has qualitative value as sample pulses were not repeated more than once per membrane or for multiple membranes of the same coating.

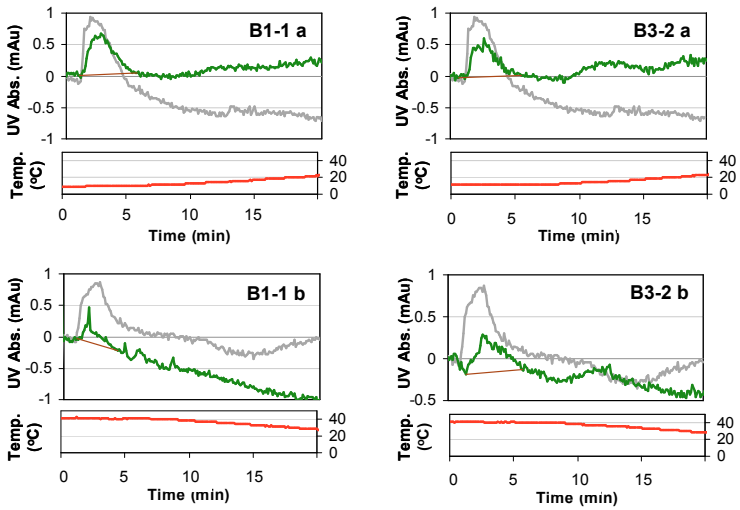

Figure 12: Insulin flow-through UV absorbance profiles for membranes B1-1 and B3-2. Both cold (a) and hot (b) temperature signals are shown for each membrane. Small elution fractions are identifiable for B1-1 a, and both B3-2 temperature conditions. The integration baselines are shown for the flow through fractions and E2 injection occurs at time = 0. A control UV absorbance signal for uncoated paper is provided in light grey for comparison in each graph.

4.3 ESEM Imaging

Environmental scanning electron microscope (ESEM) images were taken of various coated membranes as well as the uncoated Whatman filter paper. Coated membranes were imaged in the attempt to display visual differences in hydrogel dispersion, coating microstructure and coating composition. From Figure 13, ESEM imaging of the uncoated filter paper shows a high degree of cellulose fibre swelling when wet, the cellulose fibres increase in diameter with a smoothing of the fibre surface. The adhesion points between the cellulose fibres remains fixed, preventing much spatial reorientation of the fibres from their positions in the dry condition.

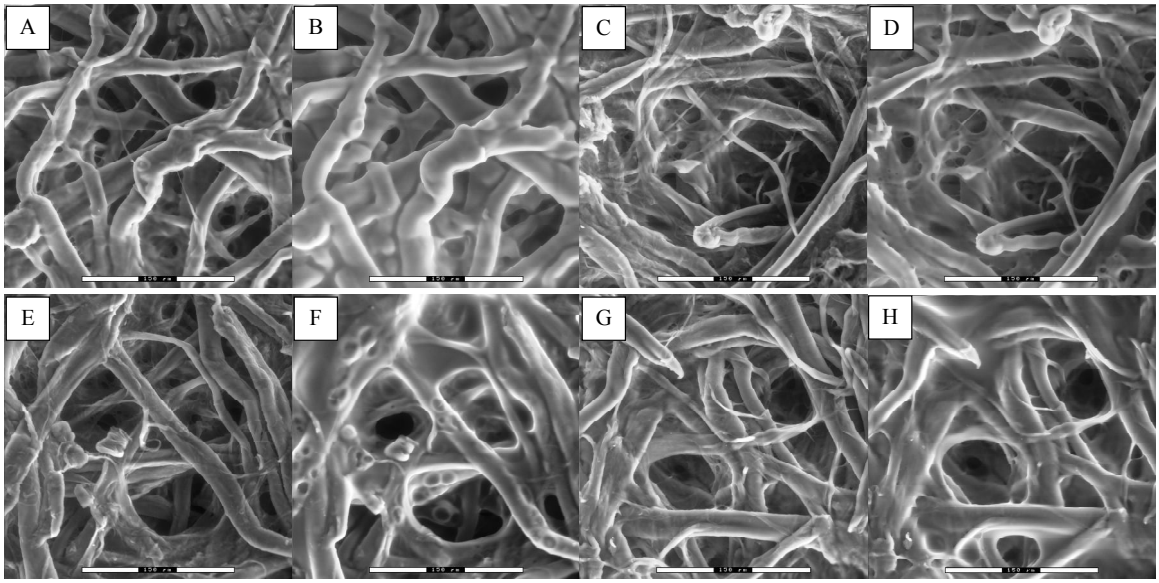

Figure 13: ESEM images of various membranes. Shown are: dry (A) and wet (B) uncoated Whatman filter paper; paper substrate coated with pre-gel formula A4-1, 10.96% mass gain, dry conditions (C) and wet conditions (D); paper substrate coated with pre-gel formula B2-1, 11.84% mass gain, dry conditions (E) and wet conditions (F); paper substrate coated with pre-gel formula B3-1, 9.33% mass gain, dry conditions (G) and wet conditions (H). All scale bars measure 150 µm.

Comparing dry states of the coated membranes and the uncoated filter paper, we can see a smoothening of the fibre surfaces with hydrogel loading, however the fibres maintain their general sizes. Distinction between thin cellulose fibres and any polymer webs is not obvious as image depth is not intuitive. Comparing wet states of the coated membranes and the uncoated filter paper, it is clear that the cellulose fibres do not change in diameter as significantly as when they are uncoated and the hydrogel loading of the cellulose network becomes clear. The hydrogel coating of the cellulose fibres clearly shows reduced pore sizes and accounts for the general reduction in permeability of coated membranes. It is not clear however, the difference between coating composition or microstructure. The random copolymer coatings appear very similar to the IPN coatings and those coatings incorporating BMA appear similar to those without. As all imaged membranes have similar mass gains regardless of coating composition, the hydrogel dispersion appears similar. It was not possible to obtain ESEM images of wetted membranes at higher temperatures due to vapour interference.

4.4 Wet Tensile Testing

Wet tensile testing was not conducted for all membrane coatings as these results are not imperative to their characterization in this work. The coated membranes that were tested

were from 2.0 M monomer basis formulations and 1.0 mol% MBAm inclusion. From that defined standard, what are comparable from the results of these tests are mechanical property differences due to BMA inclusion and coating microstructure. From Table 5 it is clear that elastic modulus is highly variable even in the uncoated filter paper and the modulus of all the coated membranes is within the range of statistical error of the control group. Only B3-3 membranes show any significant improvement but there is not enough supporting evidence to infer any cause for the improvement. The strength of the coated membranes however is clearly improved through the coating process and appears to respond to both mass gain of the filter paper and coating microstructure. Strength was not observed to respond to BMA inclusion.

Table 5: Results of wet tensile strength testing of various coated membranes.

Coating	Elastic Modulus (MPa)		Strength (MPa)		Average Mass Gain	
Control	47.74	+/- 9.43	1.061	+/- 0.170	0%	+/- 0.00%
B2-0	42.04	+/- 10.54	2.328	+/- 0.424	9.75%	+/- 1.22%
B2-3	35.19	+/- 9.77	1.773	+/- 0.366	3.81%	+/- 1.41%
A5-2	49.89	+/- 11.34	3.356	+/- 0.569	6.86%	+/- 1.45%
B3-3	64.48	+/- 6.91	4.201	+/- 0.281	9.97%	+/- 0.71%

4.5 Chapter References

1. Katime, I., et al., Theophylline release from poly(acrylic acid-co-acrylamide) hydrogels. Polymer Testing, 1999. **18**(7): p. 559-566.
2. Tanaka, T., Collapse of Gels and the Critical Endpoint. Physical Review Letters, 1978. **40**(12): p. 820.
3. Klenina, O.V. and E.G. Fain, *Phase separation in the system polyacrylic acid-polyacrylamide-water*. Polymer Science U.S.S.R., 1981. **23**(6): p. 1439-1446.
4. Aoki, T., M. Kawashima, H. Katono, K. Sanui, N. Ogata, T. Okano, Y. Sakurai, Temperature-Responsive Interpenetrating Polymer Networks Constructed with Poly(acrylic acid) and Poly(N,N-dimthylacrylamide). Macromolecules, 1994. **27**: p. 947 - 952.
5. Katono, H., et al., Thermo-responsive swelling and drug release switching of interpenetrating polymer networks composed of poly(acrylamide-co-butyl methacrylate) and poly (acrylic acid). Journal of Controlled Release, 1991. **16**(1-2): p. 215-227.

6. Yang, M., et al., Temperature-Responsive Properties of Poly(acrylic acid-co-acrylamide) Hydrophobic Association Hydrogels with High Mechanical Strength. Macromolecules, 2010. **43**(24): p. 10645-10651.
7. Ghosh, R. and T. Wong, Effect of module design on the efficiency of membrane chromatographic separation processes. Journal of Membrane Science, 2006. **281**(1–2): p. 532-540.
8. Nghiem, L.D., A.I. Schäfer, and M. Elimelech, *Removal of Natural Hormones by Nanofiltration Membranes: Measurement, Modeling, and Mechanisms.* Environmental Science & Technology, 2004. **38**(6): p. 1888-1896.
9. Ghosh, R., *Principles of Bioseparations Engineering*. 2006, World Scientific: Singapore. p. 221-223.

5. Conclusion

This study worked to develop a basis for an improved membrane technology applicable to wastewater removal of endocrine disrupting substances, in particular 17β-estradiol, a highly potent and persistent steroid hormone. This project borrows common concepts from literature but does not reproduce them in application. There are many instances of novel synthesis for thermo-responsive membranes many of which use grafting techniques with negative volume-phase transition hydrogels [1-4]. Very few studies report the synthesis of a positive thermo-responsive membrane such as is reported here [5]. There are many reports of membrane efficacy for removal of estrogens from wastewater, however all evaluate commercially available membranes, none of which were stimuli-responsive [6-12].

The qualities of a membrane that were considered in order to evaluate improvement were: hydraulic productivity, the membrane must be able to handle high volume through-puts without bottlenecking processes; surface functionality, the membrane would need strong adsorption capacity to partition trace concentrations of contaminants at competitive levels to alternative methods; stimuli-responsive, partitioned contaminants must be removable with ease under controlled conditions; cost-effective, the synthesis process should be simple, requiring little energy and using widely abundant materials while remaining effectual; environmentally friendly, the developed membrane technology shouldn't compound environmental contamination problems after its utility degrades and be easy to dispose or recycle.

5.1 Membrane Coating Synthesis

The cellulose paper membranes coated with a thermo-responsive PVT hydrogel in this study displayed distinct permeability responses indicating that the swelling and collapse of the hydrogel polymerized throughout the cellulose network was able to affect the porosity of the membrane as expected. Other than hydrogel loading on the membranes, the factors examined in the synthesis of these hydrogel coatings had minimal effect on the responsive permeability of the membranes. The deviations in monomer ratio and degree of crosslinking in this work had insignificant influence. Greater perturbations in the composition of the pre-gel formulas would be needed to elucidate their effect. Incorporating BMA monomer into the hydrogel coating improved the consistency and resolution of the permeability temperature response. Inclusion less than 3 mol% didn't significantly alter the temperature range of volume-phase transition of the coating and would most likely have more effect on the hydrophobic nature of the coating.

An increased wet tensile strength was the only mechanical benefit of forming a composite membrane through this coating process with IPN coating being stronger than their random copolymer counterparts. The elastic modulus of the substrate is much greater than that of the hydrogel leaving the composite effects on modulus negligible.

5.2 Adsorption Testing

All membranes tested reduced the amount of E2 injected through the membrane by cold temperature adsorption. This was apparent in the difference between injection and flow-through quantities. This was taken to signify that some retention of E2 had occurred and in some instances, an elution fraction was also observed as temperature was changed. The sample of E2 that was used had a higher concentration than typical environmental concentrations to aid in the measurement of absorbance signals. The adsorbed mass per membrane area as effective binding capacity was reported to indicate the quantity of available binding sites. Comparable adsorptive membrane technologies have achieved effective binding capacities between 0.12 and 0.30 μg/cm2 [7-9, 12]. The membrane fabricated in this work performed in the top half of that range and occasionally exceeding it. A few of the thermo-responsive IPN membranes synthesized in this work were also able to produce an elution fraction within the given filtration volume. While more time-consuming to synthesize, the better distributed functional groups in the IPN hydrogel coating enabled better adsorption performance at lower required mass loading. The apparent irreversible adsorption of E2 and insulin at both hot and cold temperatures by various membranes infers that the coated membranes are capable of strong hydrogen bonding with E2. A larger absorbance signal was frequently detected from hot temperature E2 injections that suggesting excess material was being rejected from the membrane as a delayed elution fraction, questioning the apparent irreversible adsorption earlier. Larger filtration volumes from longer flow times at sustained elevated temperatures were most likely responsible for a delayed elution of bound E2 resulting in an absorbance signal augmentation not possibly observed at earlier filtration volumes. E2 adsorption due to hydrogen bonding is probable and would be stable until the higher temperatures reached in this study. Hydrophobic interaction was most strongly indicated by the E2 reduction from hot state injections to the 5 mol% BMA content membranes. Hydrophobic interaction of the membranes beyond the capacity of BMA content is only simulated at lower temperatures due to the hydrogel's preference to interface with itself instead of with water when collapsed. This hydrogen bond driven self-aggregation is then broken at elevated temperatures and the hydrogel favourably interacts with water. Any persistent adsorption is unlikely to be hydrophobic bonding with this specific hydrogel coating. Adsorption of insulin on the membranes appeared to support the existence of hydrophobic interactions at colder temperatures but the high retentions at warm

temperature indicates size exclusion and discredits any evidence from the insulin binding tests.

5.3 Result Evaluation

The thermo-responsive membranes developed in this study achieved mixed results on the evaluation criteria outline above. The coated membranes displayed permeability much higher than all nanofiltration or reverse osmosis membranes reviewed for similar purposes, signifying a higher hydraulic productivity by requiring less feed pressure to produce a higher flow rate. The coated membranes displayed obvious thermo-responsiveness exemplified by the pore size gating mechanism controlling permeability. The coating process successfully utilized a filter paper substrate with an acrylamide polymer, both abundant and inexpensive materials, whose functionality was proven reversible with the same membrane over several cycles. Paper is a naturally biodegradable material and polyacrylamide degrades without releasing monomer (see below). The surface functionality of the membranes was highly inconsistent however, and being a key aspect to the viability of this new membrane technology, prevents the project from clearly being successful. Some membrane formulations did perform well, giving promise to the hypothesis of this project that an adsorption based thermo-responsive membrane is possible for the removal of estrogens. The membranes developed for this study better proved the viability of the synthesis process but gave preliminary membranes whose mixed binding capabilities leave room for future work.

The contaminant removal method of the membranes developed in this project differs from the majority of similar research in that it does not rely on a pressure driven sieving mechanism. Certain coated membranes tested were shown to have strong potential for temperature driven reversible adsorption. While the reversibility of solute adsorption is still in need of optimisation, the feasibility of such a technique as a passive adsorbent or an active barrier has been strengthened, not discredited.

5.3.1 Additional Remarks

Partitioning of well-known hydrophobic molecules may not be a strong quantitative method of determining hydrophobic potential of these smart membranes, it provides clear insight into any hydrophobic functional of the membranes. Other common techniques such as contact angle measurement and equilibrium adsorption isotherms to determine a binding coefficient could be misleading or impractical for the content of this study. Contact angle is a measure of hydrophobicity, and hydrogen bonding was determined to be the most likely dominant mechanism for these membranes, and adsorption isotherms are overly difficult and time consuming for evaluation of a system with dynamic temperature and solute concentration. Most publications of similar work therefore do not

evaluate a binding coefficient or water contact angle. Although the reversible binding of E2 doesn't consistently occur with Am and AA based hydrogel-coated membranes, constant evident of adsorption is encouraging for further research like optimizing coating composition, polymerization method and using salt-free mobile phases.

Acrylamide monomer is a potent toxin while polyacrylamide has very low toxicity. Proper polymerization and washing techniques remove most toxic residues and polyacrylamide is highly unlikely to degrade into its monomer at environmental conditions [13-15]. While adequate polymerization or washing procedures may not have been used to ensure negligible toxic leaching in this project, the basis of the developed membrane is environmentally safe.

Competitive adsorption with natural organic mater has been addressed by other researchers working with membranes in water treatment [8-11]. There are differing views on the matter but the most recent findings indicate that adsorption of contaminants onto organic matter increases the retention of the contaminants by membranes from size exclusion. However natural organic matter can be a significant source of fouling in large concentrations, especially with small-pore membranes.

5.4 Recommendations

As mentioned, the various hydrogel coating compositions examined in this project gave mixed adsorption results. Optimization of the coating composition to increase both the maximum strength of the hydrophobic interaction and hydrogen bonding capability as well as the reversibility of those functionalities should be performed. This can be done either by adjusting the content of monomers already present or substituting acrylamide for other similarly structured monomers, like methacrylamide. Also, the few membranes that did produce an elution fraction did so at fairly low temperatures. Refining the content of transition temperature adjusting monomers such as butylmethacrylate can raise the temperature where elution occurs.

While the focus of this project was on 17β-estradiol, many other EDSs readily found in wastewater have similar hydrogen bonding or hydrophobic interaction attributes. Specific feasibility studies utilizing real or simulated wastewater should be completed with a cocktail of EDS contaminants.

Conclusive results concerning membrane fouling were not obtained while performing experiments with the synthesized coated membranes. For full characterization of the performance of these membranes, focus should be given to the extent and effect of fouling. Lifespan of the membranes was not explicitly examined in this project but it was roughly determined that the thermo-responsive function of the membranes deteriorated

after approximately fourteen thermal cycles. The lifespan of similar thermo-responsive membranes are rarely reported.

5.5 Chapter References

1. Chu, L.-Y., et al., Control of pore size and permeability of a glucose-responsive gating membrane for insulin delivery. Journal of Controlled Release, 2004. 97(1): p. 43-53.
2. Park, Y.S., Y. Ito, and Y. Imanishi, Permeation Control through Porous Membranes Immobilized with Thermosensitive Polymer. Langmuir, 1998. 14(4): p. 910-914.
3. Yang, M., et al., Thermo-Responsive Gating Characteristics of Poly(N-isopropylacrylamide)-Grafted Membranes. Chemical Engineering & Technology, 2006. 29(5): p. 631-636.
4. Zhang, K. and X.Y. Wu, Temperature and pH-responsive polymeric composite membranes for controlled delivery of proteins and peptides. Biomaterials, 2004. 25(22): p. 5281-5291.
5. Chu, L.-Y., et al., Negatively Thermoresponsive Membranes with Functional Gates Driven by Zipper-Type Hydrogen-Bonding Interactions. Angewandte Chemie International Edition, 2005. 44(14): p. 2124-2127.
6. Han, J., W. Qiu, and W. Gao, Adsorption of estrone in microfiltration membrane filters. Chemical Engineering Journal, 2010. 165(3): p. 819-826.
7. Nghiem, L.D., et al., Estrogenic hormone removal from wastewater using NF/RO membranes. Journal of Membrane Science, 2004. 242(1–2): p. 37-45.
8. Nghiem, L.D., A.I. Schäfer, and M. Elimelech, Removal of Natural Hormones by Nanofiltration Membranes: Measurement, Modeling, and Mechanisms. Environmental Science & Technology, 2004. 38(6): p. 1888-1896.
9. Schäfer, A.I., L.D. Nghiem, and T.D. Waite, Removal of the Natural Hormone Estrone from Aqueous Solutions Using Nanofiltration and Reverse Osmosis. Environmental Science & Technology, 2003. 37(1): p. 182-188.
10. Yangali-Quintanilla, V., et al., Proposing nanofiltration as acceptable barrier for organic contaminants in water reuse. Journal of Membrane Science, 2010. 362: p. 334.
11. Yoon, Y., et al., Nanofiltration and ultrafiltration of endocrine disrupting compounds, pharmaceuticals and personal care products. Journal of Membrane Science, 2006. 270(1–2): p. 88-100.

12. Nghiem, L.D., A.I. Schäfer, and T.D. Waite, Adsorptive interactions between membranes and trace contaminants. Desalination, 2002. 147(1–3): p. 269-274.
13. Reber, A.C., S.N. Khanna, and R. Ottenbrite, Thermodynamic stability of polyacrylamide and poly(N,N-dimethyl acrylamide). Polymers for Advanced Technologies, 2007. 18(12): p. 978-985.
14. Caulfield, M.J., et al., Degradation on polyacrylamides. Part I. Linear polyacrylamide. Polymer, 2003. 44(5): p. 1331-1337.
15. Caulfield, M.J., et al., Degradation on polyacrylamides. Part II. Polyacrylamide gels. Polymer, 2003. 44(14): p. 3817-3826.